Downloaded from http://sp.lyellcollection.org/ at University of Sydney on May 1, 2015

Late Mesozoic mafic magmatism from the North China Block: constraints on chemical and isotopic heterogeneity of the subcontinental lithospheric mantle

W.-M. FAN[1], F. GUO[1], Y.-J. WANG[1] & H.-F. ZHANG[2]

[1]*Key Laboratory of Marginal Sea Geology, Guangzhou Institute of Geochemistry, Chinese Academy of Sciences, Wushan, Guangzhou, 510640, China (e-mail: wmfan@cashq.ac.cn)*

[2]*Institute of Geology and Geophysics, Chinese Academy of Sciences, Beijing, 100029, China*

Abstract: Available major, trace element and Sr–Nd isotope data for the late Mesozoic mafic rocks in the eastern North China Block (NCB) show chemical and isotopic differences between rocks from different tectonic units. Such differences are interpreted as signatures inherited from the melted mantle sources, which had experienced distinctive enrichment processes during lithospheric evolution. The subcontinental lithospheric mantle beneath the NCB interior is characterized by long-term light REE (LREE) enrichment and EM1-like Sr–Nd isotopic signatures. Such a lithospheric mantle is mainly composed of chemically refractory peridotites that are common in cratonic regions. In contrast to that of the NCB interior, beneath the northern part of the NCB a relatively chemically fertile mantle was enriched in large ion lithophile elements and LREE and depleted in Nb–Ta and Th–U. It has higher $^{87}Sr/^{86}Sr(i)$ and $\varepsilon_{Nd}(t)$ than that of the interior of the block, and is interpreted to have been modified by recycled lower continental crust components related to the palaeo-Asian Ocean subduction. The lithospheric mantle beneath the southern NCB has the highest $^{87}Sr/^{86}Sr(i)$ and the lowest $\varepsilon_{Nd}(t)$, and is chemically transitional between the interior and northern part of the block. Formation of such an enriched lithospheric mantle was closely associated with modification from the subducted Yangtze lower–middle crust during Triassic collision between the North China and Yangtze Blocks. A lithospheric extension–thinning model is proposed to explain the petrogenesis of these late Mesozoic mafic rocks in the eastern North China Block. This process was amplified by effects from surrounding plate interactions, including the rapid northward movement of the palaeo-Pacific Ocean, compressional forces from the Siberian plate, the Tethyan tectonic belt and possibly the Indo-China Block. The resultant forces triggered lithospheric extension, asthenospheric upwelling, and decompressional melting of the enriched mantle sources.

The nature of the subcontinental lithospheric mantle (SCLM) is important for understanding the Earth's evolution and basalt petrogenesis. It is widely considered that certain kinds of mantle reservoirs correspond to regional tectonic settings (e.g. Hart 1988; Boyd 1989; Menzies 1989). For instance, beneath cratonic regions such as the Kaapvaal, Siberia, Wyoming and Slave Cratons (Walker *et al.* 1989; Carlson & Irving 1994; Pearson *et al.* 1995; Griffin *et al.* 1999), the lithospheric mantle is generally characterized by low Rb/Sr and Sm/Nd as well as an I-type enriched mantle (EM1)-like isotopic signature. A II-type enriched mantle (EM2)-like mantle reservoir is located beneath circum-cratonic terranes, where crustal material had been recycled into the mantle through plate subduction (Boyd 1989), whereas there are mid-ocean ridge basalt (MORB) and ocean island basalt (OIB) types of mantle reservoirs beneath tectonically mobile Phanerozoic belts (Menzies 1989). However, some tectonically remobilized regions, such as the eastern North China Block (NCB) underwent decoupling between crustal rocks and subcrustal mantle. The NCB is one of the oldest continents, with recorded crustal ages of *c*. 3.8 Ga (Liu *et al.* 1992). In contrast, the present lithospheric mantle is mainly composed of chemically fertile spinel peridotite with a lithospheric thickness of 70–80 km, similar to that beneath oceanic plates or Phanerozoic mobile belts (e.g. Griffin *et al.* 1992, 1998; Menzies *et al.* 1993; Fan *et al.* 2000). Comparative studies of mantle xenoliths hosted in early Ordovician diamondiferous kimberlites and Cenozoic alkaline basalts suggest a loss of >100 km of lithospheric mantle during the last 400 Ma (Fan & Menzies 1992; Griffin *et al.* 1992, 1998; Menzies *et al.* 1993; Chi & Lu 1996; Wang *et al.* 1998; Fan *et al.* 2000; Xu 2001; Zheng *et al.* 2001). Such a thinning process has attracted the interest of international geologists, and several tectonic models have been proposed to explain the transformation of the early Palaeozoic subcratonic mantle lithosphere (180–220 km, within the diamond stability field) into the Cenozoic

From: ZHAI, M.-G., WINDLEY, B. F., KUSKY, T. M. & MENG, Q. R. (eds) *Mesozoic Sub-Continental Lithospheric Thinning Under Eastern Asia*. Geological Society, London, Special Publications, **280**, 77–100. DOI: 10.1144/SP280.4
0305-8719/07/$15 © The Geological Society of London 2007.

Downloaded from http://sp.lyellcollection.org/ at University of Sydney on May 1, 2015

MORB–OIB-type mantle (e.g. Fan & Menzies 1992; Menzies *et al.* 1993; Gao *et al.* 1998, 2004; Fan *et al.* 2000; Xu 2001; Zheng *et al.* 2001).

As an intermediate stage of lithospheric evolution, the Mesozoic lithospheric mantle holds the key to the following questions: (1) What kind of mantle reservoir was predominantly removed? (2) How did the lithospheric thinning process proceed? Because of the paucity of Mesozoic mantle xenoliths, many geologists have carried out geochemical investigations on the widespread late Mesozoic mafic igneous rocks in the NCB (e.g. Jahn *et al.* 1999; Fan *et al.* 2001, 2004; Guo *et al.* 2001, 2003, 2004, 2005*a*, *b*, 2007; Shao *et al.* 2001; Zhou *et al.* 2001; Zhang *et al.* 2002, 2003, 2004; Wilde *et al.* 2003; Chen *et al.* 2004; Li *et al.* 2004; Yang *et al.* 2004; Wang *et al.* 2005, 2006; Zhao *et al.* 2005). On the whole, all these late Mesozoic mafic rocks show arc-like trace element features with large ion lithophile element (LILE) and light REE (LREE) enrichments and high field strength element (HFSE) depletion, and low radiogenic Nd with variably radiogenic Sr isotopic compositions. Such features are widely considered to be inherited from LILE- and LREE-enriched mantle sources (e.g. Jahn *et al.* 1999; Fan *et al.* 2001, 2004; Guo *et al.* 2001, 2003, 2004, 2005*a*; Zhang *et al.* 2002, 2003, 2004; Li *et al.* 2004; Wang *et al.* 2005, 2006). Nevertheless, there still exist chemical and isotopic differences between rocks from the various tectonic units. In this paper, we compile the available data for major and trace elements and Sr–Nd isotopes of these mafic rocks from the various tectonic units of the NCB. Our aim is to: (1) understand the chemical and isotopic heterogeneity of the SCLM and the possible enrichment processes; and (2) propose a tectonic model to interpret the extensional tectonics that were responsible for the extensive magmatism in the NCB.

Geological background

The eastern NCB is bordered by the Triassic Qinling–Dabie–Sulu collisional orogen in the south and by the late Palaeozoic to early Mesozoic Central Asian Orogenic Belt (CAOB) in the north (Fig. 1; e.g. Davis *et al.* 2001). To the east is the NE Asian active continental margin related to the Pacific Ocean subduction. It is separated from the western NCB by the central high-pressure granulite zone, which formed in the early Proterozoic (Zhao 2001). The NCB has experienced a multiple-stage crustal evolution history; the Archaean to early Proterozoic was the most important (e.g. Liu *et al.* 1992; Zhai *et al*. 2000). High-grade metamorphic rocks are widely exposed, emplaced by extensive hypersthene granites and tonalite–trondhjemite–granites of 2.4–2.5 Ga (e.g. Zhai *et al*. 2000). At *c*. 1.8 Ga, collision between the western and eastern blocks formed a north–south-trending high-pressure granulite belt (e.g. Zhao 2001). The Archaean to early Proterozoic tectonic evolution created the framework of the metamorphic basement.

A Mesoproterozoic passive rift (the Yan-Liao Rift) in the northern part of the NCB is characterized by carbonate and clastic terrestrial sediments tens of kilometres thick (e.g. the Changcheng, Jixian and Qingbaikou Systems; Hebei Bureau of Geology and Mineral Resources 1988). The rift had closed by the end of the Mesoproterozoic. From the Neoproterozoic to early Palaeozoic the NCB was a passive continental margin, where neritic carbonates thousands of metres thick were deposited. The eruption of diamond-bearing kimberlites and their mantle xenoliths suggests that the NCB was a tectonically stable block in the early Palaeozoic. A gap in sedimentation from the Late Ordovician to the Early Carboniferous marks a major period of uplift of the continent. In the Permo-Triassic, collision between the NCB and the Mongolian Block created the southern segment of the CAOB (Sëngor *et al.* 1993; Xiao *et al.* 2003), and the Triassic collision between the NCB and Yangtze Block formed the Qinling–Dabie–Sulu orogen in the south (e.g. Li *et al.* 1993).

The early Mesozoic geology of the NCB is characterized by intracontinental compression and orogeny (e.g. Li 1994; Davis *et al.* 2001). Several workers have suggested that in the northern and southern NCB, sporadic emplacement of mafic to felsic magmas along the lithosphere-scale faults occurred as a consequence of local lithospheric extension or slab breakoff (Davis *et al.* 2001; Chen *et al.* 2003; Li *et al.* 2004; Guo *et al.* 2007). In contrast, magmatic activity was absent in the NCB interior. In the late Mesozoic lithospheric extension was dominant across the NCB, accompanied by emplacement of voluminous magmas of ultramafic–mafic to felsic composition, extensive gold mineralization, and formation of NE–SW- to NNE–SSW-trending fault-bound sedimentary basins. Such a sequence of geological events has been widely attributed to thinning of the NCB lithosphere either by removal of a lithospheric root beneath the main orogens or by convective thinning of ancient subcratonic lithospheric mantle (e.g. Fan *et al.* 2001, 2004; Guo *et al.* 2001, 2003; Xu 2001; Zhang *et al.* 2004).

The lithospheric thinning reached its maximum in the early Tertiary, especially around the Bohai Bay, where asthenosphere-derived tholeiitic basalts were erupted; Xu *et al.* (1995) estimated that the

Downloaded from http://sp.lyellcollection.org/ at University of Sydney on May 1, 2015

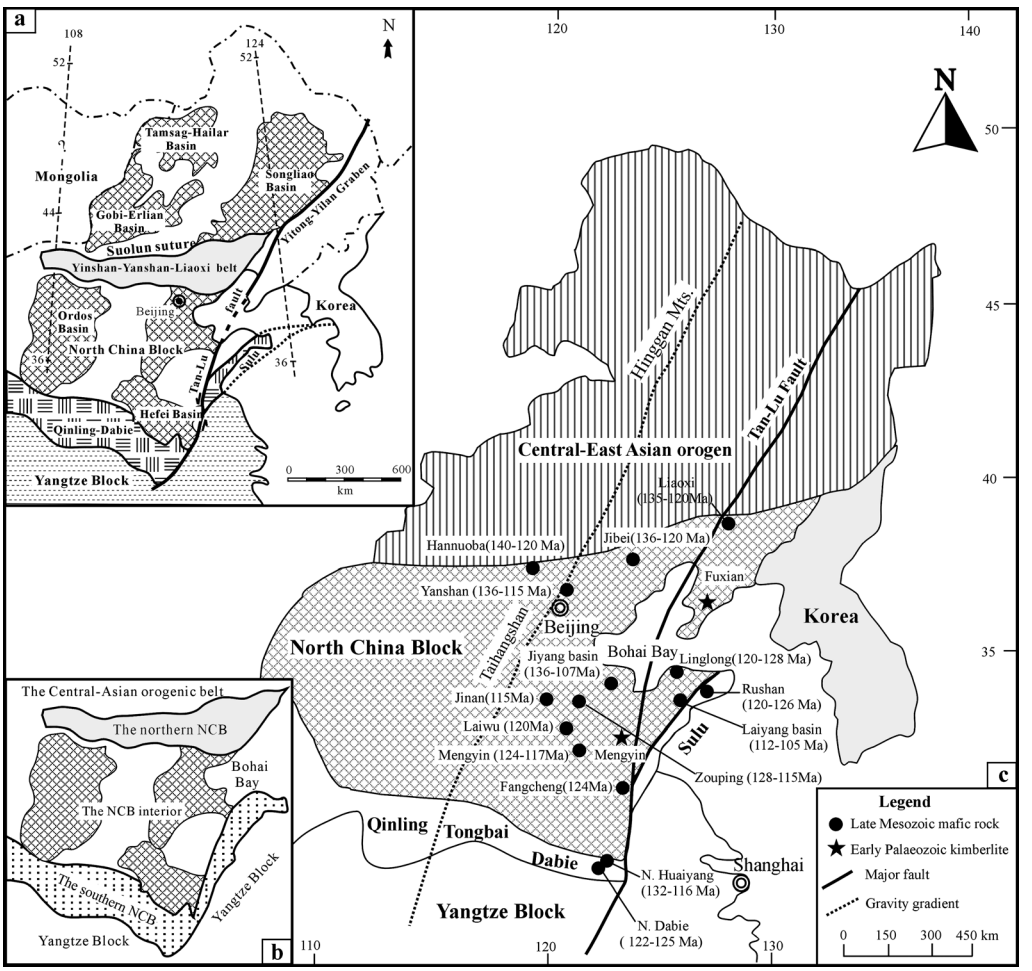


Fig. 1. A simplified geological map of the North China Block, showing the distribution of the late Mesozoic mafic rocks. The isotopic ages of the late Mesozoic mafic rocks are from Table 1.

lithospheric thickness was 55–70 km. Thermal decay of upwelling asthenosphere and lithospheric accretion took place as a result of melt extraction, and led to the Neogene–Quaternary extrusion of widespread xenolithic alkaline basalts.

Geochronology of Mesozoic mafic magmatism in NCB

We subdivide the NCB into three tectonic units from north to south: (1) the northern unit, which includes the Yinshan–Yanshan–Liaoxi tectono-magmatic belt, where Mesozoic magmatic activity began in the early Jurassic (e.g. Davis *et al.* 2001; Li *et al.* 2004; Guo *et al.* 2007); (2) the interior, mainly in the Taihangshan and Luxi areas; (3) the southern margin, which includes regions along the Triassic Qingling–Dabie–Sulu collisional orogen (Fig. 1b).

Widespread late Mesozoic mafic rocks in the NCB include (Fig. 1) intrusive ultramafic–mafic complexes, (e.g. Jinan, Zouping and Taihanshan in the NCB interior; Guo *et al.* 2001; Zhang *et al.* 2004; Wang *et al.* 2005*b*), the Dabie terrane in the southern NCB (Jahn *et al.* 1999; Li *et al.* 1999; Zhao *et al.* 2005), and mafic dykes and lavas all over the NCB (Fan *et al.* 2001, 2004; Shao *et al.* 2001; Zhou *et al.* 2001; Guo *et al.* 2004, 2005*a*, *b*; Yang *et al.* 2004; Wang *et al.* 2005). Available K–Ar, Ar–Ar and U–Pb zircon dating of these mafic rocks indicates that their emplacement age

Downloaded from http://sp.lyellcollection.org/ at University of Sydney on May 1, 2015

spanned a range from 140 to 105 Ma with a peak around 125 Ma. The isotopic ages of late Mesozoic mafic rocks in the NCB are summarized in Table 1.

Petrology of late Mesozoic mafic rocks in the NCB

The late Mesozoic NCB mafic rocks comprise a wide spectrum of rock types, including ultramafic cumulates (e.g. pyroxenites), gabbros, diorites, lamprophyres, basalts, trachybasalts, basaltic andesites and trachyandesites. Their country rocks comprise the Archaean–early Proterozoic metamorphic basement, Triassic HP–UHP metamorphic terranes, and Mesoproterozoic to Mesozoic sediments.

A cumulate texture is characteristic of the ultramafic–mafic intrusions, such as in the Jinan norites and the pyroxenites in the Dabie terrane. Most mafic extrusive rocks, such as the mafic lavas and dykes and lamprophyres, show a porphyritic texture with predominant phenocrysts of clinopyroxene, plagioclase and subordinate olivine, and amphibole in basaltic andesites and trachyandesites. The gabbros and gabbroic diorite generally show a mosaic texture with euhedral to subhedral shapes of the major phases such as plagioclase, clinopyroxene and amphibole. The main petrographic features of the late Mesozoic NCB mafic rocks are summarized in Table 2.

Geochemistry of late Mesozoic mafic rocks in the NCB

Major elements

On a loss on ignition-free basis, the late Mesozoic NCB mafic rocks have large ranges of SiO_2 (41–57%) and MgO (2.5–19%), with lower MgO in the northern NCB rocks. Some ultramafic samples from the southern region and interior of the NCB that have a cumulate texture (e.g. norites from the Jinan intrusion and pyroxenites from the Dabie terrane (Table 2; Jahn *et al.* 1999; Guo *et al.* 2001; Zhao *et al.* 2005) are mafic cumulates. These rocks generally have higher MgO and CaO, and lower Al_2O_3, K_2O, Na_2O and P_2O_5 (Fig. 2). Strictly, cumulates cannot represent mantle-derived magmas but are assemblages of early fractional phases, and their elemental features are mainly controlled by the major minerals. Therefore, we will avoid using these rocks to discuss the magmatic processes and source characteristics in the following text.

All late Mesozoic NCB mafic rocks show a general increase in SiO_2, Al_2O_3, K_2O and P_2O_5, and decrease in FeO_T, CaO and CaO/Al_2O_3 following a decrease in MgO. Rocks from the southern region and interior of the NCB also show an increase in Na_2O and TiO_2, whereas the northern NCB samples show random variation in Na_2O and TiO_2. At a given MgO the northern NCB rocks generally have higher TiO_2 and P_2O_5 than the others, and the NCB interior rocks have the lowest TiO_2 and P_2O_5.

Trace elements

To avoid effects caused by fractional crystallization and/or crustal contamination, we selected those samples free of a cumulate texture to calculate the average abundances of mafic rocks from each locality. Primitive mantle-normalized trace element spidergrams of mafic rocks from various localities are shown in Figure 3. All mafic rocks from the NCB have LILE and LREE enrichments but HFSE depletion, similar to modern arc basalts or contaminated continental flood basalts (e.g. Grove & Kinzler 1986; Peng *et al.* 1994), but completely different from asthenosphere-derived magmas (e.g. MORB and OIB; Fig. 3; Sun & McDonough 1989).

There are still some trace element differences between the mafic rocks from the various units of the NCB. For instance, the NCB interior rocks have lower La, at about 40 times that of primitive mantle, whereas other samples from the northern and southern NCB span a range of La that is 80–200 times that of primitive mantle. Additionally, the NCB interior samples show a trough in Zr–Hf with respect to Sm and Eu, whereas samples from the northern NCB exhibit Th–U depletion relative to Ba and La.

Sr–Nd isotopes

Sr–Nd isotope data of the late Mesozoic NCB mafic rocks are listed in Table 3 and plotted in Figure 4. All rocks have variably radiogenic Sr but unradiogenic Nd isotopic compositions, spanning a range of $^{87}Sr/^{86}Sr(i)$ from 0.7040 to 0.7104 and $\varepsilon_{Nd}(t)$ from −19.2 to −5.4, completely different from that of the Cenozoic basalts ($^{87}Sr/^{86}Sr(i) = 0.703 - 0.705$ and $\varepsilon_{Nd}(t) = -3$ to $+6$) in eastern China (e.g. Liu *et al.* 1994). In addition, there are considerable Sr–Nd isotopic differences among rocks from the various tectonic units. In general, the southern NCB rocks have the highest $^{87}Sr/^{86}Sr(i)$ and lowest $\varepsilon_{Nd}(t)$ values, whereas the NCB interior samples have the lowest $^{87}Sr/^{86}Sr(i)$, but relatively lower $\varepsilon_{Nd}(t)$ than the northern NCB rocks. Nevertheless, even samples from the same tectonic unit also show fairly variable Sr–Nd isotopic compositions (Table 2 and Fig. 4).

Downloaded from http://sp.lyellcollection.org/ at University of Sydney on May 1, 2015

Table 1. *A summary of isotopic ages of the NCB late Mesozoic mafic rocks*

Locality	Rock type	Age (Ma)	Method	References
NCB interior				
Jinan	Hyperite–norite–gabbro–diorite intrusion	115	Ar–Ar	Lin *et al.* 1996
Zouping	Gabbro–diorite intrusion	115	Ar–Ar	Lin *et al.* 1996
Zouping	Basaltic trachyandesite	128–130	K–Ar	Guo *et al.* 2003
Jiyang basin	Basalts and andesites	136–107	K–Ar	This study
Laiwu	Gabbro and diorite	120	Rb–Sr	Chi *et al.* 1994
Taihangshan	Gabbro and diorite	122–125	Zircon, U–Pb	Wang *et al.* 2005*b*
Northern NCB				
Liaoxi	Mafic volcanic lavas	135–120	K–Ar, Ar–Ar	Chen *et al.* 1997
Yanshan	Mafic dykes	124	K–Ar	Shao *et al.* 2001
Yanshan	Mafic volcanic lavas	136–115	K–Ar, Ar–Ar	Davis *et al.* 2001
Hannuoba	Mafic granulites and metagabbros	140–120	Zircon, U–Pb	Fan *et al.* 1998; Wilde *et al.* 2003; Liu *et al.* 2004
Southern NCB				
Fangcheng	Olivine basalt	125	K–Ar	Zhang *et al.* 2002
North Huaiyang	Mafic volcanic rocks	132–116	K–Ar	Fan *et al.* 2004
Dabie terrane	Ultramafic–mafic intrusions	122–125	Zircon, U–Pb, Ar–Ar	Jahn *et al.* 1999; Li *et al.* 1999; Zhao *et al.* 2005
Dabie terrane	Mafic dykes	132–125	Ar–Ar	Wang *et al.* 2005*a*
Laiyang basin	Mafic volcanic rocks	105–112	K–Ar	Guo *et al.* 2005*a*
Jiaodong	Lamprophyres and mafic dykes	121–125	K–Ar	Guo *et al.* 2004; Yang *et al.* 2004

Downloaded from http://sp.lyellcollection.org/ at University of Sydney on May 1, 2015

Table 2. *A summary of petrographic features of the late Mesozoic NCB mafic rocks*

Locality	Rock type	Texture	Mineral assemblage/phenocryst	Basement rocks
NCB interior				
Jinan	Norite–gabbro–diorite	Gabbroic fabrics and cumulate texture	Ol + Opx + Cpx + Pl +Bi + accessories	Palaeozoic carbonates
Zouping	Gabbro and diorite	Gabbroic fabrics	Ol + Opx + Cpx + Pl + Bi + Q + accessories	Palaeozoic carbonates
	Basaltic trachyandesites	Porphyritic texture	Ol (minor) + Cpx + Pl + Amph	Palaeozoic carbonates
Taihangshan	Gabbro and diorite	Mosaic texture and gabbroic fabrics	Ol + Cpx + Pl + amph + accessories	Metamorphic basement
Jiyang Basin	Basalt and andesite	Porphyritic fabrics	Ol + Cpx + Pl	Mesozoic sediments
Northern NCB				
Xishan	Basaltic trachyandesite	Porphyritic fabrics	Cpx + Pl+ Amph	Mesozoic sediments
	Mafic dyke	Porphyritic fabrics	Ol + Cpx + Pl + Bi	Mesozoic sediments
Jibei	Trachybasalt and basaltic trachyandesite	Porphyritic fabrics	Cpx + Pl + amph	Mesozoic sediments
Liaoxi	High-Mg andesite	Porphyritic fabrics	Ol + Cpx + Pl	Mesozoic sediments
Hannuoba	Mafic granulite and metagabbro	Granulitic and cumulate texture	Opx + Cpx + Pl + Q	Hosted by Cenozoic basalts
Southern NCB				
Dabie terrane	Pyroxenite, gabbro and diorite	Cumulate texture and gabbroic fabrics	Ol + Opx + Cpx + Pl + Amph + accessories	Dabie metamorphic complex
	Mafic dyke	Porphyritic fabrics	Cpx + Pl + amph	North Dabie complex, Mesozoic sediments
	Basaltic trachyandesite	Porphyritic fabrics	Cpx + Pl + amph	Mesozoic sediments
Sulu belt	Trachybasalt and trachyandesite	Porphyritic fabrics	Ol + Cpx + Pl + amph	Mesozoic sediments
	Lamprophyre	Porphyritic fabrics	Ol + Cpx + Pl + Kf + Bi + Amph	Metamorphic terranes

Ol, olivine; Opx, orthopyroxene; Cpx, clinopyroxene; Amph, amphibole; Bi, biotite; Pl, plagioclase; Kf, potassium feldspar; Q, quartz. Data sources are the same as in Table 1.

Downloaded from http://sp.lyellcollection.org/ at University of Sydney on May 1, 2015

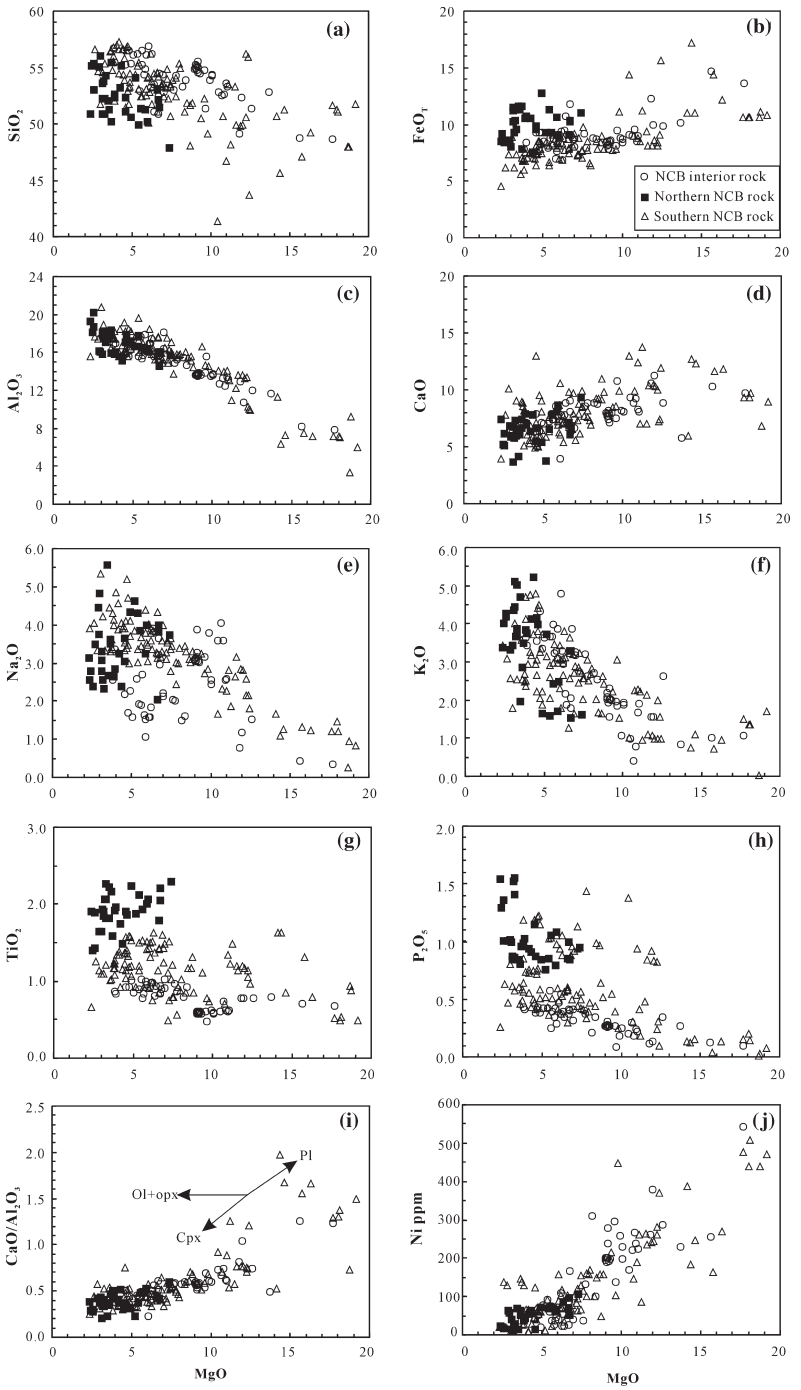


Fig. 2. MgO v. major element oxide (in wt%) (**a**–**h**) and CaO/Al_2O_3 (i) and Ni (in ppm) (**j**) diagrams of the late Mesozoic NCB mafic rocks. Data for the NCB interior are from Guo *et al.* (2001, 2003), Chen *et al.* (2004), Zhang *et al.* (2004) and Wang *et al.* (2005*b*); for the northern NCB from Shao *et al.* (2001), Zhou *et al.* (2001) and Guo *et al.* (2007); and for the southern NCB from Jahn *et al.* (1999), Fan *et al.* (2001, 2004), Zhang *et al.* (2002), Guo *et al.* (2004, 2005*a*), Yang *et al.* (2004), Wang *et al.* (2005*a*) and Zhao *et al.* (2005).

Downloaded from http://sp.lyellcollection.org/ at University of Sydney on May 1, 2015

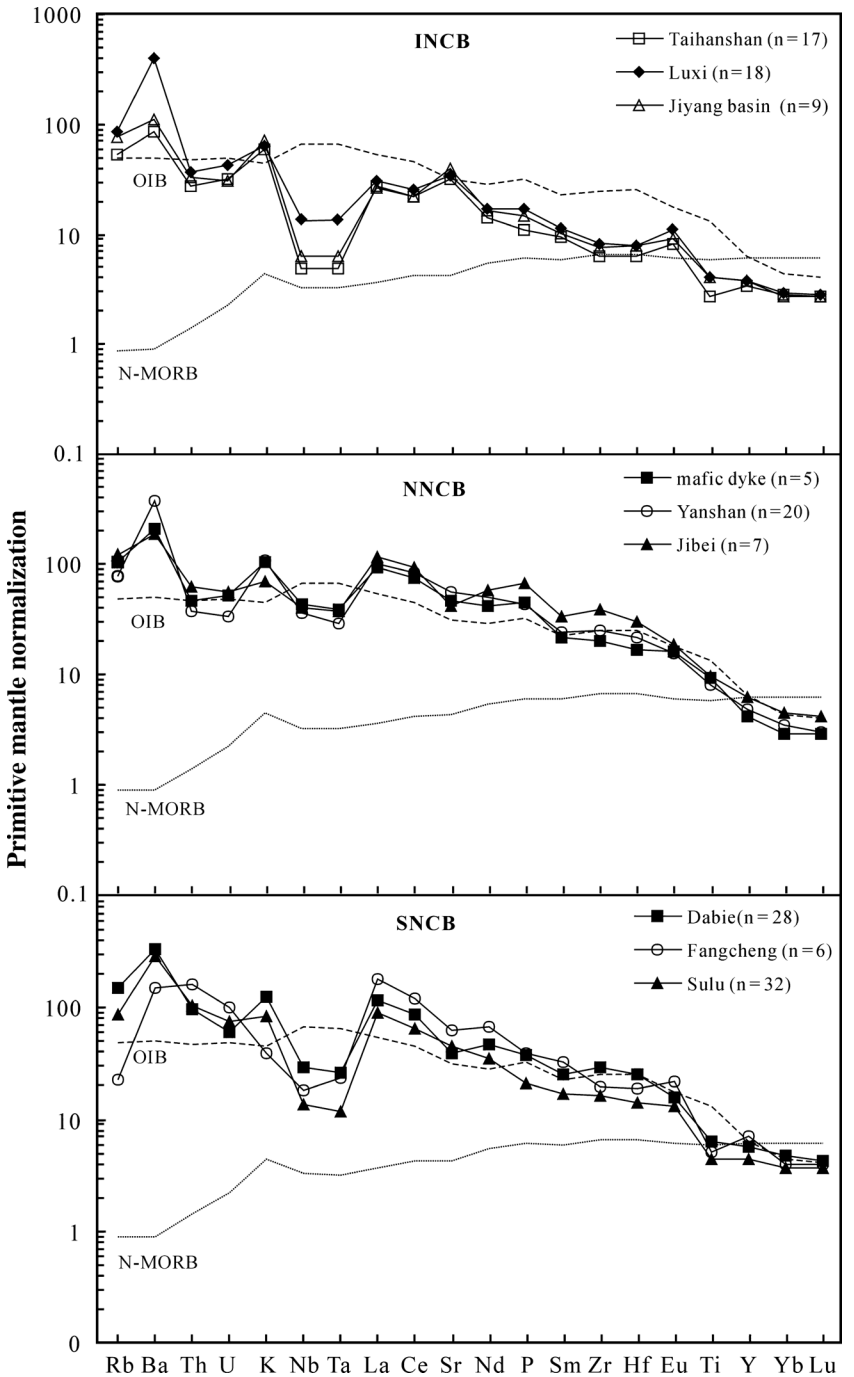


Fig. 3. Primitive mantle-normalized trace element spidergrams of the late Mesozoic mafic rocks from different tectonic units of the NCB. Normalized values for primitive mantle are from Sun & McDonough (1989). Data sources are same as in Figure 2. INCB, NNCB and SNCB refer to the interior, northern and southern NCB.

Table 3. *Sr–Nd isotope compositions of the NCB late Mesozoic mafic rocks*

Tectonic unit	Sample number	Lithology	$^{87}Sr/^{86}Sr(i)$	$\varepsilon_{Nd}(t)$	References
Northern NCB					
Liaoxi–Jibei	18	Mafic lavas and high-Mg andesites	0.7061–0.7069	−9.0 to −6.0	Zhou *et al.* 2001; Zhang *et al.* 2003; Guo *et al.* 2007
Hannuoba	18	Mafic granulites and metagabbros	0.7059–0.7086	−18.2 to −9.0	Zhang *et al.* 1998; Zhou *et al.* 2002
Yanshan	9	Mafic lavas and dykes	0.7053–0.7069	−14.1 to −7.2	Shao *et al.* 2001; Zhou *et al.* 2001; Guo *et al.* 2007
NCB interior					
Jinan–Zouping	20	Mafic intrusions and mafic lavas	0.7042–0.7058	−18.7 to −6.1	Guo *et al.* 2001, 2003; Zhang *et al.* 2004
Taihangshan	18	Gabbros and gabbroic diorites	0.7049–0.7054	−16.6 to −11.2	Chen *et al.* 2004; Wang *et al.* 2005*a*
Jiyang basin	8	Basalts and basaltic andesites	0.7041–0.7049	−13.9 to −5.4	Our unpublished data
Southern NCB					
North Dabie terrane	30	Mafic intrusions, dykes and basaltic lavas	0.7070–0.7092	−19.2 to −13.9	Jahn *et al.* 1999; Fan *et al.* 2004; Wang *et al.* 2005*b*
Sulu belt	25	Basaltic lavas and lamprophyres	0.7072–0.7091	−18.2 to −15.5	Fan *et al.* 2001; Guo *et al.* 2004, 2005*a*
Jiaodong	10	Mafic dykes	0.7075–0.7114	−17.2 to −11.0	Yang *et al.* 2004
Fangcheng	6	Olivine basalts	0.7096–0.7101	−13.1 to −14.2	Zhang *et al.* 2002

Downloaded from http://sp.lyellcollection.org/ at University of Sydney on May 1, 2015

Downloaded from http://sp.lyellcollection.org/ at University of Sydney on May 1, 2015

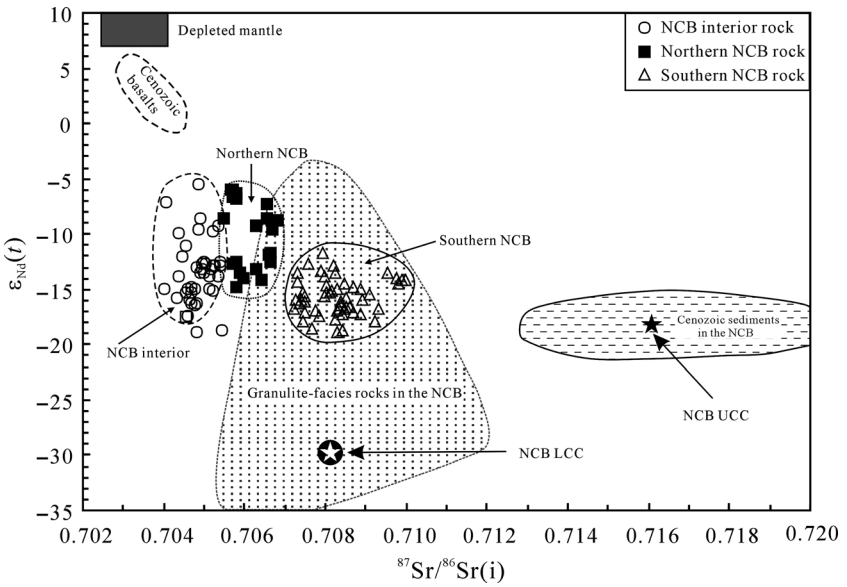


Fig. 4. Sr–Nd isotope data of late Mesozoic mafic rocks from the NCB. Data for the Cenozoic NCB sediments are our unpublished data; data for granulite-facies xenoliths are from Zhang *et al.* (1998), Zhou *et al.* (2002), Huang *et al.* (2004) and Li *et al.* (2004); and those for the Cenozoic basalts of eastern China are compiled from Liu *et al.* (1994). The other data sources are same as in Figure 2. UCC, upper continental crust; LCC, lower continental crust.

Chemical and isotopic heterogeneity of the SCLM beneath the NCB

Possible effect of crustal contamination

Before using the available geochemical data to constrain the source characteristics of the melted mantle sources, it is necessary to evaluate the effect of crustal contamination or assimilation–fractional crystallization (AFC) during magma evolution, because all late Mesozoic NCB mafic rocks have significant negative Nb–Ta anomalies in primitive mantle-normalized spidergrams, radiogenic Sr and unradiogenic Nd isotopic compositions. Mass balance considerations suggest that such features cannot be realistically attributed to crustal contamination or AFC of asthenosphere-derived magmas such as MORB and OIB. As shown by Figure 5a, addition of 40–60% upper continental crust (UCC) or lower continental crust (LCC) to OIB-type magma would produce the observed Sr–Nd isotopic compositions in the NCB mafic rocks. Introduction of such high proportion of crustal material could not be re-equilibrated with a heat budget. The Sr–Nd isotopic compositions in these rocks could not be produced by assimilation by UCC or LCC (Fig. 5a). For instance, with a remaining magma fraction less than 0.1, LCC assimilation will create a magma with $\varepsilon_{Nd}(t)$ around −5. Such a low remaining magma fraction would lead to extensive magma fractionation and the created magma should have been felsic rather than mafic. Although some continental basalts with arc-type trace element features (e.g. some contaminated continental flood basalts and continental potassic mafic magmas) could be produced by interaction between asthenosphere-derived magma and the overlying enriched lithospheric mantle (e.g. Arndt & Jenner 1986; Peng *et al.* 1994; O'Brien *et al.* 1995; Shimizu *et al.* 2005), the absence of contemporaneous MORB- or OIB-type mafic magmas across the block tends to rule out this possibility. We thus consider that the geochemical features in the NCB mafic rocks were mainly derived from enriched lithospheric mantle.

The Sr isotope ratios in the southern and northern NCB mafic rocks are generally higher than those in rocks from the NCB interior: such a difference could have been produced by crustal contamination or AFC. We selected the possible endmember components and partition coefficients (K_D) for Sr and Nd to model this possibility. As shown by Figure 5b, for a magma with $^{87}Sr/^{86}Sr(i)$ at 0.704 and $\varepsilon_{Nd}(t)$ at −7, an addition of >50% UCC into such a magma would produce a new melt similar to the lowest $^{87}Sr/^{86}Sr(i)$ (*c.* 0.707) in the southern NCB rocks. AFC modelling results show that it is necessary for the remaining magma fraction of <0.2 to produce a magma with $^{87}Sr/^{86}Sr(i)$ *c.* 0.707. Neither LCC contamination

Downloaded from http://sp.lyellcollection.org/ at University of Sydney on May 1, 2015

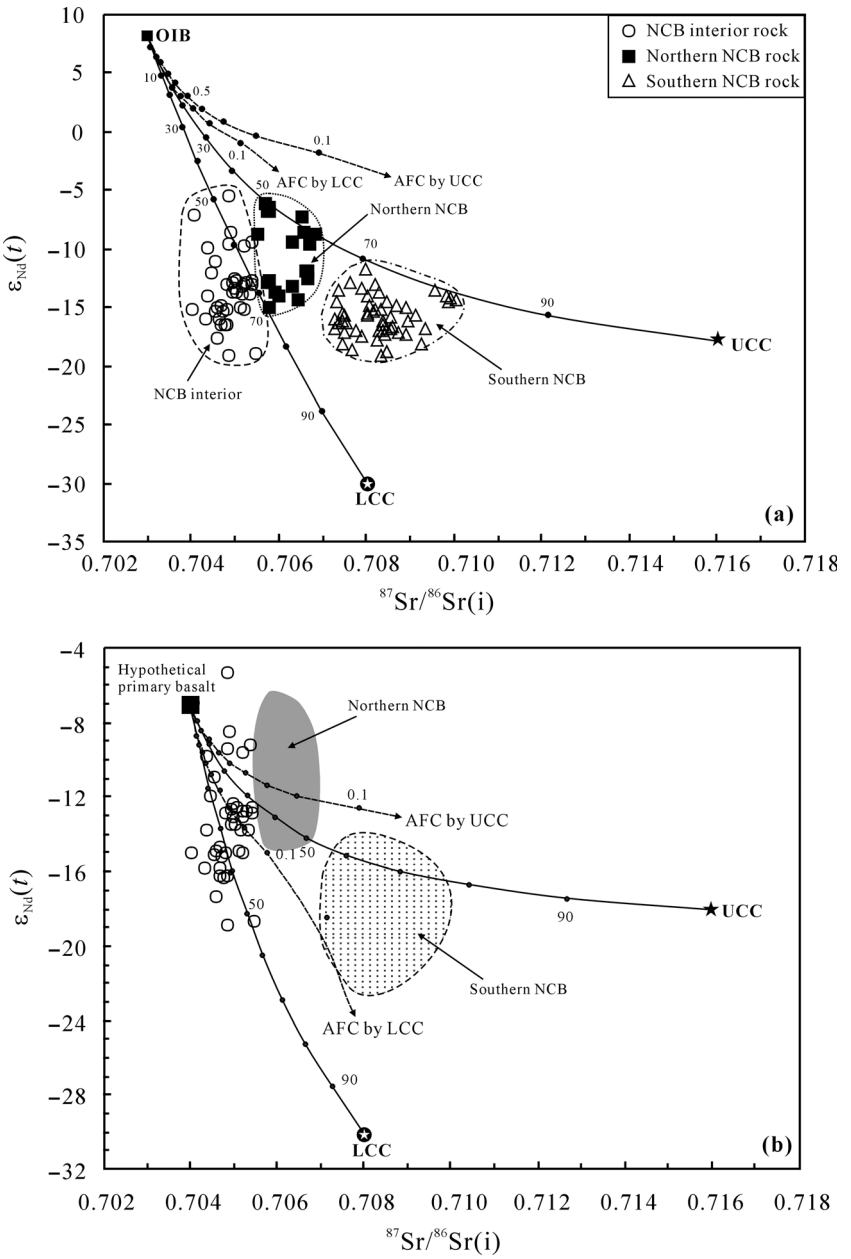


Fig. 5. Sr–Nd isotopic modelling results of the effect of crustal contamination and AFC on the late Mesozoic NCB mafic rocks. In (**a**) is shown crustal contamination and AFC of an assumed OIB-type basalt, and of a hypothetical primary basalt from the NCB interior. The assimilation rate is assumed to be 0.25, $K_D^{Sr} = 1.2$, $K_D^{Nd} = 0.5$. Dashed lines represent AFC curves and continuous lines denote bulk mixing curves between the hypothetical primary basalt and crustal components. The NCB UCC composition is compiled from the Cenozoic NCB sediments (our unpublished data), and the NCB LCC composition is compiled from data for the granulite xenoliths and Archaean high-grade metamorphic terranes in the NCB of Jahn & Zhang (1984), Zhang *et al.* (1998), Zhou *et al.* (2002), Huang *et al.* (2004) and Liu *et al.* (2004). The hypothetical primary basalt is a basaltic sample from the Jiyang basin in the NCB interior (our unpublished data). The composition of OIB is arbitrarily assumed. Tick marks on the AFC curves represent increments of 0.1 of the remaining magma fraction, and those on the bulk mixing curves denote the percent of the mixed crustal component. The other calculation parameters used for Sr–Nd isotopic modelling are listed below:

Downloaded from http://sp.lyellcollection.org/ at University of Sydney on May 1, 2015

Component	Sr (ppm)	Nd (ppm)	$^{87}Sr/^{86}Sr(i)$	$\varepsilon_{Nd}(t)$
OIB	800	35	0.703	+8
UCC	210	40	0.716	−18
LCC	350	20	0.708	−30
Hypothetical primary basalt	923	27	0.704	−7

nor assimilation can produce the Sr isotopic difference between the interior and the southern NCB rocks. The northern NCB mafic rocks, which have slightly higher $^{87}Sr/^{86}Sr(i)$ than the NCB interior samples, could not be simply interpreted as the contamination or AFC products of the NCB interior mafic magmas. Sr–Nd isotopic modelling results suggest that either an addition of 30% UCC into a magma with $^{87}Sr/^{86}Sr(i)$ at 0.704 or UCC assimilation with the remaining magma fraction of around 0.4 could create the lowest $^{87}Sr/^{86}Sr(i)$ (*c*. 0.7055) sample from the northern NCB (Fig. 3b). Nevertheless, the northern NCB mafic rocks show considerable Th–U depletion relative to Ba and La; some samples even have a Th/La ratio lower than that of N-MORB (Guo *et al.* 2007). Such trace element features call for either contamination or assimilation by lower crustal rocks (Rudnick & Fountain 1995). Increase of $^{87}Sr/^{86}Sr(i)$ from 0.704 to 0.7055 required either addition of >50% LCC to the hypothetical primary magma or LCC assimilation with the remaining magma fraction of <0.1. Similarly, both mass balance and heat considerations argue against an origin of these melts by LCC contamination or assimilation of the primary melts from the NCB interior. Accordingly, the difference in Sr–Nd isotopes between the mafic rocks from different units was mainly inherited from heterogeneous mantle sources.

The effect of crustal contamination and AFC on the mafic rocks from individual localities has been discussed in previous studies (e.g. Jahn *et al.* 1999; Fan *et al.* 2001, 2004; Guo *et al.* 2001, 2004, 2005*a*, *b*, 2007; Zhou *et al.* 2001; Zhang *et al.* 2002, 2003, 2004; Yang *et al.* 2004; Wang *et al.* 2005, 2006; Zhao *et al.* 2005). Using various methods, they proved that the majority of the NCB mafic rocks had escaped significant crustal contamination through their extrusion or intrusion. In the following discussion, we will select those samples free of contamination and cumulate texture and having MgO >5% from the southern region and interior of the NCB. For the purpose of comparison and because of the existence of only a few samples with MgO >5% in the northern NCB, the rocks with a MgO range of 4–5% from this unit are also used for discussion.

Major element constraints

The majority of samples from both the southern region and interior of the NCB show an increase of SiO_2, Al_2O_3, K_2O, Na_2O, TiO_2 and P_2O_5, and a decrease of FeO_T, CaO, CaO/Al_2O_3 and Ni following magma differentiation, indicating a dominant fractionation of olivine and clinopyroxene (Fig. 2). However, the northern NCB rocks show an increase of SiO_2, Al_2O_3, K_2O and P_2O_5, and a decrease of TiO_2, FeO_T, CaO, CaO/Al_2O_3 and Ni following magma evolution, suggesting a fractional assemblage of olivine + clinopyroxene ± amphibole ± ilmenite.

An approach commonly used for comparison of large mafic rock datasets is to extrapolate the less evolved rocks back to 8% MgO using a best-fit linear regression. Using this method, Klein & Langmuir (1987) first identified the global trends of MORB to estimate the melting conditions, such as pressure, temperature and degree of partial melting. This has been widely applied to continental flood basalt petrogenesis and yielded important information about melting conditions and source characteristics (e.g. Turner & Hawkesworth 1995; Garland *et al.* 1996; Xu *et al.* 2001). Extrapolation of the late Mesozoic NCB mafic rocks to 8% MgO was carried out by fitting a simple correlation line, following the method and rationale of Turner & Hawkesworth (1995). Only samples with a MgO range of 5–10% from the interior and southern NCB and those with MgO >4% from the northern NCB are regressed. The correlations between MgO and SiO_2, FeO_T, TiO_2 and Na_2O of the late Mesozoic mafic rocks from different units of the NCB are illustrated in Figure 6, and the calculation results of Si_8, Fe_8, Na_8 and Ti_8 are shown in Figure 7.

The northern NCB samples have the highest Fe_8, Ti_8 and Na_8 and the lowest Si_8 of the NCB mafic rocks, and they show negative correlations between Si_8, Fe_8 and Ti_8. In contrast, the NCB interior samples have the lowest Ti_8 and Na_8 and the highest Si_8, and the southern NCB mafic rocks have Si_8, Fe_8, Ti_8 and Na_8 between those of the NCB northern and interior rocks.

Experimental melting results show that the Fe content of a melt is positively correlated with

Downloaded from http://sp.lyellcollection.org/ at University of Sydney on May 1, 2015

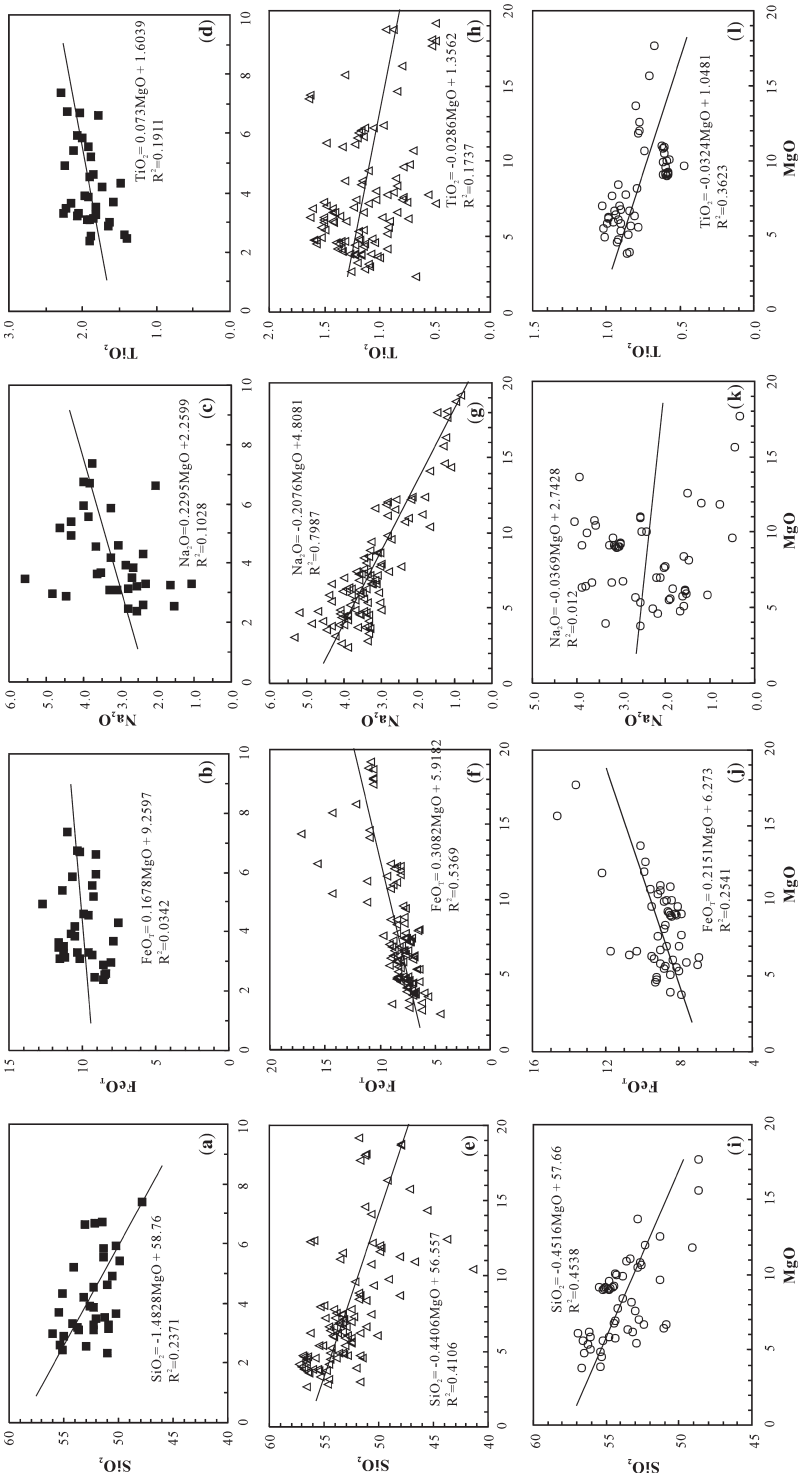


Fig. 6. Correlations between MgO and SiO_2, FeO_T, Na_2O and TiO_2 of the late Mesozoic mafic rocks from different units of the NCB. (**a–d**) The northern NCB rocks; (**e–h**) the southern NCB rocks; (**i–l**) the NCB interior rocks. Data sources are as in Figure 2.

Downloaded from http://sp.lyellcollection.org/ at University of Sydney on May 1, 2015

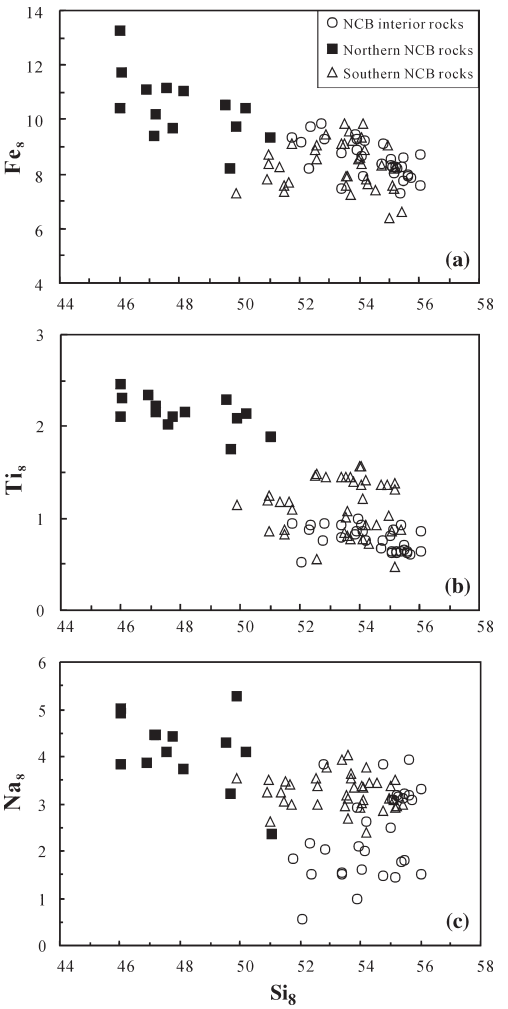


Fig. 7. Si_8 v. Fe_8, Ti_8 and Na_8 plots of the late Mesozoic NCB mafic rocks. Numbers of samples: 14 from the northern NCB; 31 from the NCB interior; 39 from the southern NCB.

pressure and source composition, and thus melts either at high pressures or derived from a fertile source will have high Fe (e.g. Kushiro 1990; Hirose & Kushiro 1993; Baker & Stolper 1994). In contrast to Fe, the Si content is negatively correlated with melting pressure, and it increases in a water-saturated system. The Ti content of a melt is a means of gauging source fertility, as it is incompatible during melting and sensitive to melt removal. Na mainly reflects the degree of melting as it acts as a moderately incompatible element in mantle conditions. However, Na is less incompatible, as it is retained in the residue and incorporated in the jadeite component of clinopyroxene at high pressures. Comparing the experimental results (e.g. Kushiro 1990; Hirose & Kushiro 1993; Baker & Stolper 1994), the highest Fe_8 and lowest Si_8 in the northern NCB mafic rocks suggest their derivation from high-pressure melting, and the highest Ti_8 and Na_8 could be caused by low degrees of partial melting. However, a different melting condition is not a unique interpretation for the compositional distinction between the mafic rocks from different units. Melt generation from a refractory mantle source can lower Fe_8, and the Ti_8 gap between the northern NCB rocks and the other samples from the NCB suggests that the northern NCB mafic magmas were derived from a more fertile mantle source than that from which the southern and interior NCB melts were derived (Fan & Guo 2005). The distinction between these alternatives is not straightforward and will be addressed in the following sections.

Trace element constraints

As previously described, some late Mesozoic mafic rocks from different tectonic units have trace element differences. Here we present a comparison to uncover possible differences between the mantle sources from which these magmas were derived. Because all late Mesozoic NCB mafic rocks discussed here had a predominant fractional assemblage of olivine and clinopyroxene, trace elemental ratios such as LILE/LREE, Th/U, Th/La and Th/Nb changed only slightly, because of the low and similar partition coefficients of these elemental pairs between the fractional phases and basaltic melts; nor would partial melting change these elemental ratios significantly. The key trace element features of the late Mesozoic mafic magmas are listed in Table 4 and plotted in Figure 8.

As shown by Figure 8, the northern NCB rocks are characterized by the lowest Th/La, Th/Nb and La/Nb, and moderate La and La/Sm. The NCB interior rocks have higher Ba/La and Sr/Nd but lower La, La/Sm, $(Zr/Sm)_N$ and $(Hf/Sm)_N$ than the others in the NCB, whereas the southern NCB samples have the highest Th, U, Th/U, La and La/Sm, and the largest range of La/Nb and Th/Nb. We thus consider that such features were mainly inherited from the melting sources. Irrespective of the effect caused by degrees of melting, one may speculate that the melting source for the NCB interior rocks also had low LREE contents. The lowest Th/La and Th/Nb ratios in the northern NCB rocks suggest that they were derived from a low-Th source, whereas the southern NCB samples, which have the highest Th, U, La and La/Sm, probably originated from a source highly enriched in these elements.

Downloaded from http://sp.lyellcollection.org/ at University of Sydney on May 1, 2015

Table 4. *Key trace element features of the late Mesozoic NCB mafic magmas*

Tectonic unit	La/Nb*	Th/Nb	Th/U	Th/La	Ba/La	Sr/Nd	La/Sm	$(Zr/Sm)_N$	$(Hf/Sm)_N$
NCB interior (n = 39)	1.8–7.6 (4.2)	0.22–1.1 (0.54)	2.8–5.9 (3.9)	0.07–0.25 (0.13)	20–264 (65)	18–64 (34)	2.7–5.3 (4.3)	0.20–1.00 (0.71)	0.41–1.16 (0.83)
Northern NCB (n = 13)	1.5–3.8 (2.7)	0.08–0.16 (0.14)	2.7–6.4 (4.6)	0.04–0.08 (0.05)	13–65 (28)	8.0–27 (17)	4.8–8.0 (6.0)	0.81–1.28 (1.03)	0.70–1.07 (0.89)
Southern NCB (n = 53)	2.0–14 (5.5)	0.24–1.53 (0.71)	3.1–7.7 (5.6)	0.08–0.33 (0.13)	8.3–70 (31)	7.8–27 (17)	4.9–9.1 (7.2)	0.47–1.51 (0.97)	0.25–1.01 (0.69)

*Values in parentheses are averages of the trace element ratios.

Downloaded from http://sp.lyellcollection.org/ at University of Sydney on May 1, 2015

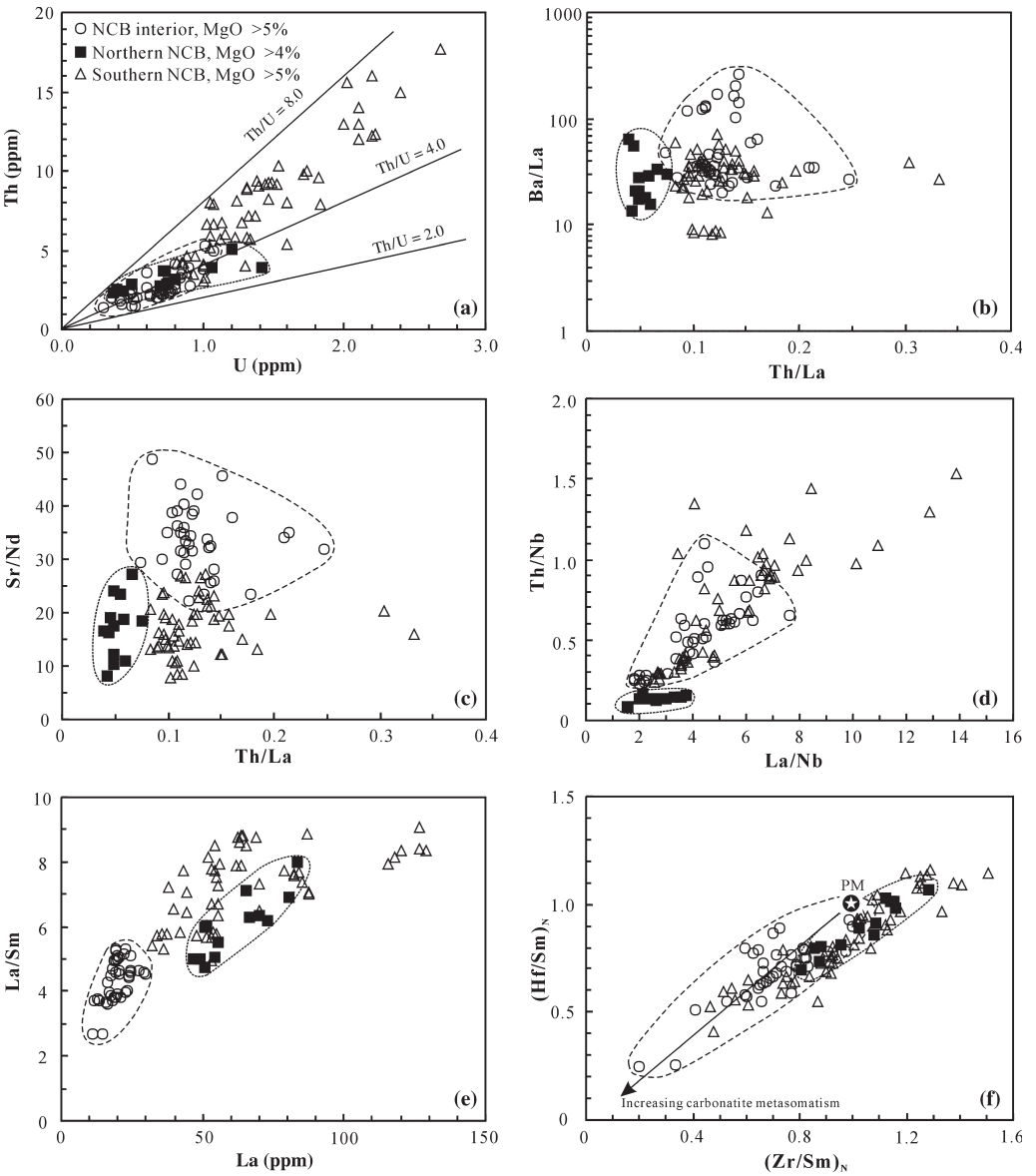


Fig. 8. Trace element plots of the NCB late Mesozoic mafic rocks. In (**a**), the southern NCB rocks have the highest Th and U, whereas samples from the interior and northern NCB have comparable Th and U contents. In (**b**) and (**c**), the NCB interior samples have the highest Ba/La and Sr/Nd ratios, and the northern NCB rocks have the lowest Th/La. In (**d**), the northern NCB rocks have lower Th/Nb and La/Nb compared with samples from the interior and southern NCB. In (**e**), the NCB interior rocks have the lowest La concentrations of the three groups and the highest La and La/Sm in the southern NCB samples. In (**f**), the NCB interior rocks have subchondritic $(Zr/Sm)_N$ and $(Hf/Sm)_N$ ratios, suggesting an important role of carbonatite metasomatism in the melting sources. Data sources are the same as in Figure 2.

Sr–Nd isotopic variations across the NCB

To show possible Sr–Nd isotopic variations across the NCB, we here compile 142 sets of Sr–Nd isotope data for the late Mesozoic mafic rocks in the NCB from the literature and our unpublished data from the Jiyang basin around the Bohai Bay. The detailed profiles are illustrated in Figure 9.

Downloaded from http://sp.lyellcollection.org/ at University of Sydney on May 1, 2015

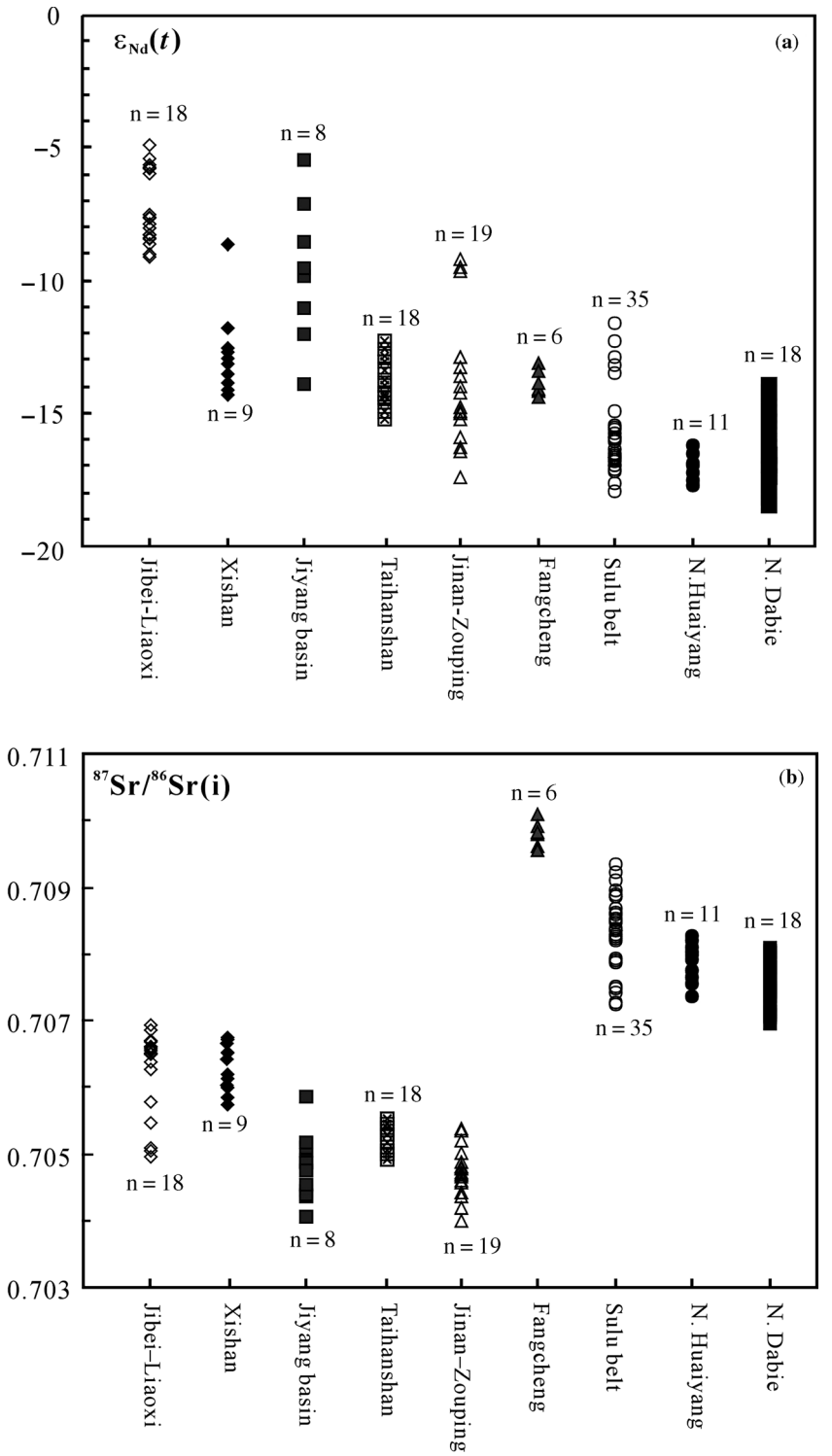


Fig. 9. Spatial Sr and Nd isotopic variations across the NCB, showing highly heterogeneous Sr and Nd isotopic compositions between different tectonic units and even between rocks from the same locality.

Downloaded from http://sp.lyellcollection.org/ at University of Sydney on May 1, 2015

There is a clear Sr–Nd isotopic heterogeneity in the mantle sources beneath the different units of the NCB. For instance, the initial $^{87}Sr/^{86}Sr(i)$ ratio ranges from *c*. 0.7065 in Jibei–Liaoxi to *c*. 0.7055 in Xishan, and to *c*. 0.7050 in the NCB interior (e.g. Jiyang basin, Taihangshan, Jinan and Zouping). From the NCB interior to the southern NCB, $^{87}Sr/^{86}Sr(i)$ increases to a maximum (>0.709) at Fangcheng, and slightly decreases from Sulu to North Huaiyang and then to the North Dabie terrane. Similarly, $\varepsilon_{Nd}(t)$ shows variations across the NCB. It is highest in the Jibei–Liaoxi region, with average values of around −8.0, and is *c*. −13 in Xishan, *c*. −14 at Taihangshan, −10 at Jiyang basin and *c*. −15 in Jinan–Zouping, and has the lowest values of around −16.5 in the Dabie–Sulu region. Despite having the highest $^{87}Sr/^{86}Sr(i)$, the Fangcheng olivine basalts have $\varepsilon_{Nd}(t)$ values of *c*. −14, somewhat higher than for other samples from the southern NCB. The highly variable Sr–Nd isotopic compositions in the late Mesozoic mafic rocks indicate highly heterogeneous mantle sources across the NCB.

Possible enrichment processes

The arc-type trace element features and enriched Sr–Nd isotopic signatures of all late Mesozoic mafic rocks from the NCB suggest that their melted mantle sources experienced LILE and LREE enrichments prior to the melting event (e.g. Menzies *et al.* 1987). Different types of melt or fluid metasomatism will create distinctive trace element and isotope compositions in metasomatized mantle (e.g. Menzies *et al.* 1987; You *et al.* 1996). For instance, a carbonatite melt or fluid has a preferential capacity to host LREE, Ba and Sr, a relatively low capacity for Rb and K, and the weakest capacity for HFSE and Ti. Therefore, a source having undergone carbonatite metasomatism would have low Rb/Sr and Sm/Nd, and HFSE and Ti depletion (Dupuy *et al.* 1992; Rudnick *et al.* 1993; Furman 1995). Slab-derived fluids preferentially host Rb, K, Ba, Sr and U, but have a low capacity for REE, Th and HFSE, so a mantle metasomatized by slab-derived fluids will have high U and Rb/Sr, and moderate Sm/Nd, and low Th and HFSE (e.g. You *et al.* 1996; Hawkesworth *et al.* 1997; Macdonald *et al.* 2000). A slab melt is characterized by TTG- or adakite-type elemental features (e.g. high Al, Na and Sr, and low Y and HREE; (Defant & Drummond 1990; Smithies 2000; Martin *et al.* 2005).

The moderate radiogenic Sr and low radiogenic Nd isotopic compositions in the NCB interior mafic rocks are similar to those derived from the SCLM beneath Archaean cratons. Such EM1-like isotopic signatures were probably caused by pervasive metasomatism of a carbonatitic melt or fluid with moderate Rb/Sr and low Sm/Nd (e.g. Menzies *et al.* 1987; Dupuy *et al.* 1992; Rudnick *et al.* 1993; Bedini *et al.* 1997; Guo *et al.* 2001; Zheng *et al.* 2005), as indicated by their higher Ba/La and Sr/Nd ratios (Fig. 8b and c) in the NCB interior mafic rocks and the occurrence of contemporaneous carbonatite magmatism in the NCB interior (e.g. Ying *et al.* 2004). It is generally considered that carbonatitic melts or fluids have a much stronger capacity to host LREE than HFSE (e.g. Dupuy *et al.* 1992; Rudnick *et al.* 1993; Guo *et al.* 2001; Zheng *et al.* 2005); a carbonatite metasomatism can also account for the considerable Zr–Hf depletion or subchondritic $(Zr/Sm)_{PM}$ and $(Hf/Sm)_{PM}$ ratios in these rocks (Figs 3a and 8f).

The northern NCB mafic rocks show spatial Sr–Nd isotopic variations. At Xishan, near the NCB interior, the mafic rocks have similar Nd isotopic ratios, and higher $^{87}Sr/^{86}Sr(i)$ ratios than those from the NCB interior, implying a recent LILE enrichment event prior to magma generation. In the Jibei–Liaoxi area, farther from the NCB interior, mafic rocks have higher $^{87}Sr/^{86}Sr(i)$ and $\varepsilon_{Nd}(t)$, signatures of subduction-related enrichment processes (e.g. You *et al.* 1996; Macdonald *et al.* 2000). Considering its high Fe_8, Ti_8 and Na_8, low Si_8, and remarkable Th–U depletion, we consider that the lithospheric mantle had been modified by recycled ancient lower crustal materials with low Th/La, probably during the late Palaeozoic–early Mesozoic Palaeo-Asian Ocean subduction (Li *et al.* 2004; Guo *et al.* 2007).

The southern NCB mafic rocks have the highest $^{87}Sr/^{86}Sr(i)$ and lowest $\varepsilon_{Nd}(t)$ of the rocks across the NCB. Such isotopic signatures suggest that the lithospheric mantle had been modified by melts or fluids with high Rb/Sr and low Sm/Nd ratios related to the Triassic collision between the NCB and Yangtze Block (Amelin *et al.* 1996; Jahn *et al.* 1999; Fan *et al.* 2001; Zhang *et al.* 2002; Guo *et al.* 2004, 2005*b*; Wang *et al.* 2005). To account for the highest Th, U and LREE concentrations in the southern NCB mafic rocks, we prefer a process of enrichment by melt metasomatism rather than fluid metasomatism, because slab-derived fluids have a low capacity to transfer Th. Based on superchondritic Zr/Nb and Th/U ratios in the mafic rocks from the Sulu belt, Guo *et al.* (2005*a*) pointed out that the melts were probably derived from diorite–trondhjemite–tonalite–granitic gneisses like those of the Kongling Group of the subducted Yangtze lithosphere (Gao *et al.* 1999; Ma *et al.* 2000). On the other hand, the moderate Nb/Ta and Zr/Hf fractionations in the majority of the southern NCB mafic rocks suggest that this enrichment process occurred at high pressures with a

Downloaded from http://sp.lyellcollection.org/ at University of Sydney on May 1, 2015

rutile- and CO_2-rich metasomatic assemblage (e.g. Guo *et al.* 2004, 2005*b*).

In summary, distinctive and diagnostic enrichment processes were responsible for the chemical and isotopic heterogeneity beneath the different tectonic units of the NCB.

Implications for the lithospheric thinning of the NCB

The late Mesozoic emplacement of voluminous mafic melts across the NCB is unique in global cratonic regions. Both numerical modelling and thermal considerations suggest that such extensive melting of lithospheric mantle requires either a voluminous heat supply or significant lithospheric extension, or both. However, evidence from geophysical surveys, the arc-like trace element patterns, and the enriched Sr–Nd isotopic signatures in these rocks argue against the presence of a plume beneath the NCB. Therefore, we attribute the extensive late Mesozoic magmatism to decompressional melting of enriched mantle sources as a consequence of lithospheric extension and thinning.

The causes of the early Cretaceous lithospheric extension of the NCB are still controversial. Wilde *et al.* (2003) correlated the lithospheric thinning event with the breakup and dispersal of Gondwanaland by a major mantle overturn, fuelled by the destruction of oceanic lithosphere and triggered by its sinking into the lower mantle during the subsequent accretion of Asia. In a lateral extrusion model, Guo *et al.* (2003) considered that tectonic forces from the compression of the Siberian plate in the north and from the Tethyan belt in the SW, together with pull-apart stresses from the rapid northward movement of the palaeo-Pacific Ocean, would have triggered lithospheric extension and formation of the regional NE–SW- to NNE–SSW-trending structure. Numerical modelling results suggest that significant thinning of a lithosphere requires a high heat flux from the convective asthenosphere, whereas tectonic stretching plays only a limited role in lithospheric attenuation (e.g. Lin *et al.* 2005). Lin *et al.* pointed that the lithospheric thinning and extensive tectonomagmatic activities in the NCB reflected the thermotectonic responses to the high heat flow responsible for the Cretaceous superplume event (Larson 1991). For instance, the production of oceanic crust in the Phanerozoic reached its peak during the early Cretaceous, and this defined a long Cretaceous normal magnetic period from 125 to 90 Ma, consistent with the eruption time of the Ontong–Java large igneous province in the southwestern Pacific Ocean (e.g. Neal *et al.* 1997). Larson (1991) proposed a superplume hypothesis to interpret the global Cretaceous event, and Filatova (1998) suggested that the formation of Cretaceous active continental margins was correlated with this global event.

Tectonic reconstruction of the eastern Asian continent indicates that the NCB was strongly affected by surrounding plate interactions (e.g. Engebretson *et al.* 1985; Faure & Natal'in 1992; Zhao *et al.* 1994; Davis *et al.* 2001). On the one hand, the NCB was dragged northward by the rapid northward movement of the palaeo-Pacific plate (e.g. Faure & Natal'in 1992; Zhao *et al.* 1994; Engebretson *et al.* 1985), which exerted a NNE–SSW-trending pull-apart stress on the NCB and its surrounding regions. Such a shearing stress led to the formation of pull-apart basins and strike-slip extension and collapse of the lithosphere (e.g. Xu *et al.* 1987; Ruppel 1995; Fan *et al.* 2001). On the other hand, the NCB was simultaneously subjected to southward and northeastward compression from the Siberian plate and the Tethyan tectonic domain, and possibly from the southern Indo-China Block, triggering a northeastward lateral escape of the NCB lithosphere (e.g. Menzies *et al.* 1993; Yin & Nie 1993; Guo *et al.* 2003; Fan & Guo 2005). The resulting tectonics, together with the global high heat flux in the early Cretaceous, caused extensive lithospheric extension and thinning of the NCB and the subsequent large-scale melting of the mantle sources (Fig. 10). As a whole, we consider that the principal late Mesozoic tectonomagmatic activities in the NCB were the intracontinental responses to surrounding plate interactions.

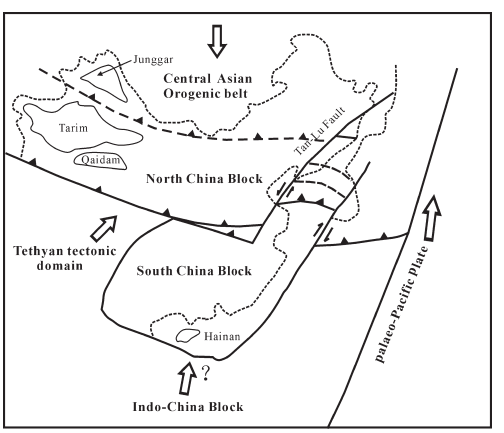


Fig. 10. A proposed tectonic model to interpret the extensive late Mesozoic tectonomagmatic activities in the NCB. This demonstrates the effects caused by surrounding plate interactions. (See details in the text.)

Downloaded from http://sp.lyellcollection.org/ at University of Sydney on May 1, 2015

Summary

Available geochemical data from the NCB late Mesozoic mafic rocks indicate that the SCLM was chemically and isotopically heterogeneous beneath different tectonic units. Such differences resulted from distinctive enrichment processes before the magma generation. The NCB interior mafic rocks have the lowest Fe_8, Na_8, Ti_8 and LREE, the highest Si_8, HFSE depletion relative to REE, and EM1-like Sr–Nd isotopic signatures. These melts were derived from a chemically refractory mantle reservoir similar to that beneath cratonic lithospheric mantle. Pervasive carbonatite metasomatism was responsible for the LREE and LILE enrichments. In contrast, the northern NCB mafic rocks have the highest Fe_8, Na_8 and Ti_8, lower Si_8, Nb–Ta and Th–U depletion, and more radiogenic Sr and Nd isotopic compositions than those from the NCB interior. These magmas originated from a chemically fertile mantle source, which had been modified by recycled lower crustal materials, possibly related to the subduction of the palaeo-Asian Ocean. The southern NCB mafic magmas are chemically transitional between the interior and northern NCB rocks, and have the highest Th, U, LREE and $^{87}Sr/^{86}Sr(i)$, and the lowest $\varepsilon_{Nd}(t)$, of the NCB samples. These melts were derived from highly LILE- and LREE-enriched mantle sources modified by subducted Yangtze lower–middle crustal rocks during the Triassic collision between the NCB and Yangtze Block.

The widespread late Mesozoic mafic magmatism in the NCB calls for a voluminous heat supply and significant lithospheric extension and thinning. Considering the global Cretaceous events that required a higher heat flux from the convective mantle, we consider that the early Cretaceous tectonomagmatic activities in the NCB were intracontinental responses to the surrounding plate interactions, which include pull-apart stresses induced by contemporaneous northward motion of the palaeo-Pacific plate and compression from the northern Siberian plate and the southwestern Tethyan belt, and possibly the South China Block.

We are grateful to N. Arndt, B. Windley and T. Komiya for their constructive comments and suggestions. This study was financially supported by the Chinese Academy of Sciences (KZCX 1-107 and GIGCX-04-04) and the National Natural Science Foundation of China (40034343).

References

AMELIN, Y. V., NEYMARK, L. A., RITSK, E. Y. & NEMCHIN, A. A. 1996. Enriched Nd–Sr–Pb isotopic signatures in the Dovyren layered intrusion (eastern Siberia, Russia): evidence for source contamination by ancient upper-crust material. *Chemical Geology*, **129**, 39–69.

ARNDT, N. T. & JENNER, G. A. 1986. Crustally contaminated komatiices and basalts from Kambalda, western Australia. *Chemical Geology*, **56**, 229–255.

BAKER, M. B. & STOLPER, E. M. 1994. Determining the compositions of high-pressure mantle melts using diamond aggregates. *Geochimica et Cosmochimica Acta*, **58**, 2811–2827.

BEDINI, R. M., BODINIER, J.-L, DAUTRIA, J.-M. & MORTEN, L. 1997. Evolution of LILE-enriched melt fraction in the lithospheric mantle: a case study from the East African Rift. *Earth and Planetary Science Letters*, **153**, 67–83.

BOYD, F. R. 1989. Composition and distinction between oceanic and cratonic lithosphere. *Earth and Planetary Science Letters*, **96**, 15–26.

CARLSON, R. W. & IRVING, A. J. 1994. Depletion and enrichment history of subcontinental lithospheric mantle: an Os, Sr, Nd and Pb isotopic study of ultramafic xenoliths from the northwestern Wyoming Craton. *Earth and Planetary Science Letters*, **126**, 457–472.

CHEN, B., JAHN, B. M., ARAKAWA, Y. & ZHAI, M. G. 2004. Petrogenesis of the Mesozoic intrusive complexes from the southern Taihang Orogen, North China Craton: elemental and Sr–Nd–Pb isotopic constraints. *Contributions to Mineralogy and Petrology*, **148**, 489–501.

CHEN, J. F., XIE, Z., LI, H. M., *ET AL.* 2003. U–Pb zircon ages for a collision-related K-rich complex at Shidao in the Sulu ultrahigh pressure terrane, China. *Geochemical Journal*, **37**, 33–46.

CHEN, Y. X., CHEN, W. J., ZHOU, X. H., ZHANG, G. H., WANG, F. & CHEN, S. H. 1997. *Geochronology, Geochemistry and Tectonic Environments of Mesozoic Volcanic Rocks in the Liaoxi and its Adjacent Areas*. Seismological Press, Beijing [in Chinese with English summary].

CHI, J. S. & LU, F. X. (eds) 1996. *Early Paleozoic Kimberlites from the North China Platform and the Affinities of the Subcontinental Lithospheric Mantle*. Science Press, Beijing, 260–264 [in Chinese].

CHI, X. G., XU, W. L., LIN, J. Q. & TAN, D. J. 1994. Nd and Sr isotopic evidence for the petrogenesis of Mesozoic dioritic intrusives in eastern North China Platform. *In*: LIN, J. Q. & TAN, D. J. (eds) *Mesozoic Potassic Magmatic Regions in the North China Platform*. Seismological Press, Beijing, 66–74 [in Chinese].

DAVIS, G. A., ZHENG, Y. D., WANG, C. & BRIAN, J. D. 2001. Mesozoic tectonic evolution of the Yanshan fold and thrust belt, with emphasis on Hebei and Liaoning province, northern China. *In*: HENDRIX, M. S. & DAVIS, G. A. (eds) *Paleozoic and Mesozoic Tectonic Evolution of Central Asia: from Continental Assembly to Intracontinental Deformation*. Geological Society of America, Memoirs, **194**, 171–197.

DEFANT, M. J. & DRUMMOND, M. S. 1990. Derivation of some modern arc magmas by melting of young subducted lithosphere. *Nature*, **347**, 662–665.

DUPUY, C., LIOTARD, J.-M. & DOSTAL, J. 1992. Zr/Hf fractionation in intraplate basaltic rocks: carbonate metasomatism in the mantle source. *Geochimica et Cosmochimica Acta*, **56**, 2417–2423.

Downloaded from http://sp.lyellcollection.org/ at University of Sydney on May 1, 2015

ENGEBRETSON, D. C., COX, A. & GORDON, R. G. 1985. Relative motions between oceanic and continental plates in the Pacific basins. Geological Society, America, Special Papers, **206**, 1–59.

FAN, Q. C., LIU, R. X. & LI, H. M. 1998. Zircon U–Pb dating and REE geochemistry of the granulite xenoliths from the Hannuoba, northern China. *Chinese Science Bulletin*, **43**, 133–137 [in Chinese].

FAN, W. M. & GUO, F. 2005. Late Mesozoic mafic magmatism from the eastern North China Block and its adjacent regions: magma genesis and geodynamic implications for lithospheric thinning. *Geotectonica et Metallogenica*, **29**, 44–55 [in Chinese with English abstract].

FAN, W. M. & MENZIES, M. A. 1992. Destruction of aged lower lithosphere and accretion of asthenosphere mantle beneath eastern China. *Geotectonica et Metallogenica*, **16**, 171–180.

FAN, W. M., ZHANG, H. F., BAKER, J., JARVIS, K. E., MASON, P. R. D. & MENZIES, M. A. 2000. On-craton and off-craton Cenozoic spinel peridotites in eastern China: similarity and difference. *Journal of Petrology*, **41**, 933–950.

FAN, W. M., GUO, F., WANG, Y. J. & ZHANG, M. 2001. Post-orogenic bimodal volcanism along the Sulu Orogenic Belt in eastern China. *Physics and Chemistry of the Earth* (*A*), **26**, 733–746.

FAN, W. M., GUO, F., WANG, Y. J. & ZHANG, M. 2004. Late Mesozoic volcanism in the northern Huaiyang tectono-magmatic belt, central China: partial melts from a lithospheric mantle with subducted continental crust relicts beneath the Dabie orogen? *Chemical Geology*, **209**, 27–48.

FAURE, M. & NATAL'IN, B. 1992. The geodynamic evolution of the eastern Eurasian margin in Mesozoic times. *Tectonophysics*, **208**, 397–411.

FILATOVA, N. I. 1998. Evolution of Cretaceous active continental margins and their correlation with other global events. *Island Arc*, **7**, 253–270.

FURMAN, T. 1995. Melting of metasomatized subcontinental lithosphere: undersaturated mafic lavas from Rungwe, Tanzania. *Contributions to Mineralogy and Petrology*, **122**, 97–115.

GAO, S., LUO, T. C., ZHANG, B. R., KERN, H. & ZHAO, Z. D. 1998. Chemical composition of the continental crust as revealed by studies in East China. *Geochimica et Cosmochimica Acta*, **62**, 1959–1975.

GAO, S., LING, W. L., QIU, Y. M., ZHOU, L., HARTMAN, G. & SIMON, K. 1999. Contrasting geochemical and Sm–Nd isotopic compositions of Archean metasediments from the Kongling high-grade terrain of the Yangtze Craton: evidence for cratonic evolution and redistribution of REE during crustal anatexis. *Geochimica et Cosmochimica Acta*, **63**, 2071–2088.

GAO, S., RUDNICK, R. L., YUAN, X. L., *ET AL*. 2004. Recycling lower continental crust in the North China Craton. *Nature*, **432**, 892–897.

GARLAND, F., TURNER, S. & HAWKESWORTH, C. 1996. Shift in the source of Paraná basalts through time. *Lithos*, **37**, 223–243.

GRIFFIN, W. L., O'REILLY, S. Y. & RYAN, C. J. 1992. Composition and thermal structure of the lithosphere beneath South Africa, Siberia and China: proton microprobe studies. *In*: *On Cenozoic Volcanic Rocks and Deep-seated Xenoliths in China and its Environments*. Abstracts of International Symposium on Cenozoic Volcanic Rocks and Deep-seated Xenoliths in China and its Environments, Beijing, pp. 65–66.

GRIFFIN, W. L., ZHANG, A. D., O'REILLY, S. Y. & RYAN, C. J. 1998. Phanerozoic evolution of the lithosphere beneath the Sino-Korean Craton. *In*: FLOWER, M. F. J., CHUNG, S. L., LO, C. H. & LEE, T. Y. (eds) *Mantle Dynamics and Plate Interactions in East Asia*, American Geophysical Union, Geodynamic Series, **27**, 107–126.

GRIFFIN, W. L., DOYLE, B. J., RYAN, C. G., *ET AL*. 1999. Layered mantle lithosphere in the Lac de Gras area, Slave Craton: composition, structure and origin. *Journal of Petrology*, **40**, 705–728.

GROVE, T. L. & KINZLER, R. J. 1986. Petrogenesis of andesites. *Annual Reviews of Earth and Planetary Sciences*, **14**, 417–454.

GUO, F., FAN, W. M., WANG, Y. J. & LIN, G. 2001. Late Mesozoic mafic intrusive complexes in North China Block: constraints on the nature of subcontinental lithospheric mantle. *Physics and Chemistry of the Earth* (*A*), **26**, 759–771.

GUO, F., FAN, W. M., WANG, Y. J. & LIN, G. 2003. Geochemistry of late Mesozoic mafic rocks in west Shandong Province: characterizing the lost lithospheric mantle beneath North China Block. *Geochemical Journal*, **37**, 63–77.

GUO, F., FAN, W. M., WANG, Y. J. & ZHANG, M. 2004. Origin of early Cretaceous calc-alkaline lamprophyres from the Sulu orogen in eastern China: implications for enrichment processes beneath continental collisional belt. *Lithos*, **78**, 291–305.

GUO, F., FAN, W. M., WANG, Y. J. & LI, C. W. 2005*a*. Petrogenesis and tectonic implications of early Cretaceous high-K calc-alkaline volcanic rocks in the Laiyang basin of the Sulu belt, eastern China. *Island Arc*, **14**, 69–90.

GUO, F., FAN, W. M., WANG, Y. J., LI, C. W., LI, X. Y. & ZHANG, H. F. 2005*b*. Geochemistry of late Mesozoic mafic rocks from the Dabie–Sulu region, China: constraints on the nature of lithospheric mantle beneath the orogen. *Acta Petrologica Sinica*, **21**, 1265–1270 [in Chinese with English abstract].

GUO, F., FAN, W.-M., LI, X.-Y. & LI, C.-W. 2007. Geochemistry of Mesozoic mafic volcanic rocks from the Yanshan belt in the northern margin of the North China Block: relations with post-collisional lithospheric extension. *In*: ZHAI, M.-G., WINDLEY, B. F., KUSKY, T. M. & MENG, Q. R. (eds) *Mesozoic Sub-continental Lithospheric Thinning Under Eastern Asia*. Geological Society, London, Special Publications, **280**, 101–129.

HART, S. R. 1988. Heterogeneous mantle domains: signature, genesis and mixing chronologies. *Earth and Planetary Science Letters*, **90**, 273–296.

HAWKESWORTH, C. J., TURNER, S., MCDERMOTT, F., PEATE, D. & VAN CALSTEREN, P. 1997. U–Th isotopes in arc magmas: implications for element transfer from the subducted crust. *Science*, **276**, 551–555.

Hebei Bureau of Geology Mineral Resources 1988. *Regional Geology of Hebei Province*. Geological Publication House, Beijing [in Chinese with English summary].

Downloaded from http://sp.lyellcollection.org/ at University of Sydney on May 1, 2015

HIROSE, K. & KUSHIRO, I. 1993. Partial melting of dry peridotites at high pressures: determination of compositions of melts segregated from peridotite using aggregates of diamond. *Earth and Planetary Science Letters*, **114**, 477–489.

HUANG, X. L., XU, Y. G. & LIU, D. Y. 2004. Geochronology, petrology and geochemistry of the granulite xenoliths from Nushan, east China: Implication for a heterogeneous lower crust beneath the Sino-Korean Craton. *Geochimica et Cosmochimica Acta*, **68**, 127–149.

JAHN, B. M. & ZHANG, Z. Q. 1984. Archean granulite gneisses from eastern Hebei Province, China: rare earth geochemistry and tectonic implications. *Contributions to Mineralogy and Petrology*, **85**, 224–243.

JAHN, B. M., WU, F. Y., LO, C.-H. & TSAI, C. H. 1999. Crust–mantle interaction induced by deep subduction of the continental crust: Geochemical and Sr–Nd isotopic evidence from post-collisional mafic–ultramafic intrusions of the northern Dabie complex, central China. *Chemical Geology*, **157**, 119–146.

KLEIN, E. M. & LANGMUIR, C. H. 1987. Global correlations of oceanic ridge basalt chemistry with axial depth and crustal thickness. *Journal of Geophysical Research*, **92**, 8089–8115.

KUSHIRO, I. 1990. Partial melting of mantle wedge and evolution of island arc crust. *Journal of Geophysical Research*, **95**, 15929–15939.

LARSON, R. L. 1991. Latest pulse of Earth: evidence for a mid-Cretaceous superplume. *Geology*, **19**, 947–950.

LI, S. G., XIAO, Y. L., LIOU, D. L., *ET AL.* 1993. Collision of the North China and Yangtze blocks and formation of coesite-bearing eclogites: timing and process. *Chemical Geology*, **109**, 89–111.

LI, S. G., HONG, J. A., LI, H. M. & JIANG, L. L. 1999. U–Pb zircon ages of the pyroxenite-gabbro intrusions in Dabie mountains and their geological implications. *Geological Journal of China Universities*, **5**, 351–355 [in Chinese with English abstract].

LI, X. Y., FAN, W. M., GUO, F., WANG, Y. J. & LI, C. W. 2004. Modification of the lithospheric mantle beneath the northern North China Block by the Paleo-Asian Ocean: geochemical evidence from the mafic volcanic rocks of the Nandaling Formation in the Xishan area, Beijing. *Acta Petrologica Sinica*, **20**, 557–566 [in Chinese with English abstract].

LI, Z. X. 1994. Collision between the North and South China Blocks: a crustal-detachment model for suturing in the region east of the Tanlu Fault. *Geology*, **22**, 739–742.

LIN, G., ZHANG, Y. H., GUO, F., WANG, Y. J. & FAN, W. M. 2005. Numerical modelling of lithosphere evolution in the North China Block: thermal versus tectonic thinning. *Journal of Geodynamics*, **40**, 92–103.

LIN, J. Q., TAN, D. J. & JIN, Y. 1996. $^{40}Ar/^{39}Ar$ ages of Mesozoic igneous rocks from west Shandong Province, China. *Acta Petrologica et Mineralogica*, **15**, 213–220 [in Chinese with English abstract].

LIU, C. Q., MASUDA, A. & XIE, G. H. 1994. Major- and trace-element compositions of Cenozoic basalts in eastern China: petrogenesis and mantle source. *Chemical Geology*, **112**, 1–20.

LIU, D. Y., NUTMAN, A. P., COMPSTON, W., WU, J. S. & SHEN, Q. H. 1992. Remnants of 3800 Ma crust in the Chinese part of the Sino-Korean craton. *Geology*, **20**, 339–342.

LIU, Y. S., GAO, S., YUAN, H. L., *ET AL.* 2004. U–Pb zircon ages and Nd, Sr, and Pb isotopes of lower crustal xenoliths from North China Craton: insights on evolution of lower continental crust. *Chemical Geology*, **211**, 87–109.

MA, C. Q., EHLERS, C., XU, C. H., LI, Z. C. & YANG, K. G. 2000. The roots of the Dabieshan ultrahigh-pressure metamorphic terrane: constraints from geochemistry and Nd–Sr isotope systematics. *Precambrian Research*, **102**, 279–301.

MACDONALD, R. & HAWKESWORTH C. J., HEATH, E. 2000. The Lesser Antilles volcanic chain: a study in arc magmatism. *Earth-Science Reviews*, **49**, 1–76.

MARTIN, H., SMITHIES, R. H., RAPP, R., MOYEN, J.-F. & CHAMPION, D. 2005. An overview of adakite, tonalite–trondhjemite–granodiorite (TTG), and sanukitoid: relationships and some implications for crustal evolution. *Lithos*, **79**, 1–24.

MENZIES, M. A. 1989. Cratonic, circum-cratonic and oceanic mantle domains beneath the western U.S.A. *Journal of Geophysical Research*, **94**, 7899–7915.

MENZIES, M. A., ROGERS, N., TINDLE, A. & HAWKESWORTH, C. J. 1987. Metasomatic and enrichment processes in lithospheric peridotites, an effect of asthenosphere-lithosphere interaction. *In*: MENZIES, M. A. & HAWKESWORTH, C. J. (eds) *Mantle Metasomatism*. Academic Press, London, 313–361.

MENZIES, M. A., FAN, W. M. & ZHANG, M. 1993. Palaeozoic and Cenozoic lithoprobes and the loss of >120 km of Archaean lithosphere Sino-Korean Craton, China. *In*: PRITCHARD, H. M., ALABASTER, T., HARRIS, N. B. W. & NEARY, C. R. (eds) *Magmatic Processes and Plate Tectonics*. Geological Society, London, Special Publications, **76**, 71–81.

NEAL, C. R., MAHONEY, J. J., KROENKE, L. W., DUNCAN, R. A. & PETTERSON, M. G., 1997. The Ontong Java Plateau. *In*: MAHONEY, J. J. & COFFIN, M. F. (eds) *Large Igneous Provinces: Continental, Oceanic, and Planetary Flood Volcanism*. Geophysical Monograph, American Geophysical Union, **100**, 183–216.

O'BRIEN, H. E., IRVING, A. J., MCCULLUM, I. S. & THIRLWALL, M. F. 1995. Strontium, neodymium, and lead isotopic evidence for the interaction of post-subduction asthenospheric potassic mafic magmas of the Highwood Mountains, Montana, USA, with ancient Wyoming craton lithospheric mantle. *Geochimica et Cosmochimica Acta*, **59**, 4539–4556.

PEARSON, D. G., SHIREY, S. B., CARLSON, R. W., BOYD, F. R., POKHILENKO, N. P. & SHIMIZU, N. 1995. Re–Os, Sm–Nd and Rb–Sr isotope evidence for thick Archean lithospheric mantle beneath the Siberian craton modified by multi-stage metasomatism. *Geochimica et Cosmochimica Acta*, **59**, 959–977.

PENG, Z. X., MAHONEY, J., HOOPER, P., HARRIS, C. & BEANE, J. 1994. A role for lower continental crust in flood basalt genesis? Isotopic and incompatible

Downloaded from http://sp.lyellcollection.org/ at University of Sydney on May 1, 2015

element study of the lower six formations of the Western Deccan Traps. *Geochimica et Cosmochimica Acta*, **58**, 267–288.

RUDNICK, R. L. & FOUNTAIN, D. M. 1995. Nature and composition of the continental crust—a lower crustal perspective. *Reviews in Geophysics*, **33**, 267–309.

RUDNICK, R. L., MCDONOUGH, W. F. & CHAPELL, B. W. 1993. Carbonatite metasomatism in the northern Tanzanian mantle: petrographic and geochemical characteristics. *Earth and Planetary Science Letters*, **114**, 463–475.

RUPPEL, C. 1995. Extensional processes in continental lithosphere. *Journal of Geophysical Research*, **100**, 24187–24215.

SËNGOR, A. M. C., NATAL'IN, B. A. & BURTMAN, V. S. 1993. Evolution of the Altaid tectonic collage and Paleozoic crustal growth in Eurasia. *Nature*, **364**, 299–307.

SHAO, J. A., LI, X. H., ZHANG, N. Q. & MOU, B. L. 2001. Petrogenesis of Mesozoic bimodal intrusive dikes at Nankou–Guyaju area in the Yanshanian Orogen, northern North China Block: Sr–Nd isotopic constraints. *Geochimica*, **30**, 517–524 [in Chinese with English abstract].

SHIMIZU, K., NAKAMURA, E. & MARUYAMA, S. 2005. The geochemistry of ultramafic to mafic volcanics from the Belingwe Greenstone Belt, Zimbabwe: magmatism in an Archaean continental large igneous province. *Journal of Petrology*, **46**, 2367–2394.

SMITHIES, R. H. 2000. The Archaean tonalite–trondhjemite–granodiorite (TTG) series is not an analogue of Cenozoic adakites. *Earth and Planetary Science Letters*, **182**, 115–125.

SUN, S. S. & MCDONOUGH, W. F. 1989. Chemical and isotopic systematics of oceanic basalts: implication for mantle composition and processes. *In*: SAUNDER, A. D. & NORRY, M. J. (eds) *Magmatism in the Ocean Basins*. Geological Society, London, Special Publications, **42**, 313–345.

TURNER, S. & HAWKESWORTH, C. J. 1995. The nature of the continental mantle lithosphere: constraints from the major element compositions of continental flood basalts. *Chemical Geology*, **120**, 295–314.

WANG, W. Y., TAKAHASHI, E. & SUENO, S. 1998. Geochemical properties of lithospheric mantle beneath the Sino-Korean craton: evidence from garnet xenocrysts and diamond inclusions. *Physics of the Earth and Planetary Interiors*, **107**, 249–260.

WANG, Y. J., FAN, W. M., PENG, T. P., ZHANG, H. F. & GUO, F. 2005. Nature of the Mesozoic lithospheric mantle and tectonic decoupling beneath the Dabie Orogen, Central China: evidence from $^{40}Ar/^{39}Ar$ geochronology, elemental and Sr–Nd-Pb isotopic compositions of early Cretaceous mafic rocks. *Chemical Geology*, **220**, 165–189.

WANG, Y. J., FAN, W. M., ZHANG, H. F. & PENG, T. P. 2006. Early Cretaceous gabbroic rocks from the Taihang Mountains: implications for a paleosubduction-related lithospheric mantle beneath the central North China Craton. *Lithos*, **86,** 281–302.

WALKER, R. J., CARLSON, R. W. & SHIREY, S. B. 1989. Os, Sr, Nd and Pb isotope systematics of southern African peridotite xenoliths: implications for the chemical evolution of subcontinental mantle. *Geochimica et Cosmochimica Acta*, **53**, 1583–1595.

WILDE, S. A., ZHOU, X.-H., NEMCHIN, A. A. & SUN, M. 2003. Mesozoic crust–mantle interaction beneath the North China craton: a consequence of the dispersal of Gondwanaland and accretion of Asia. *Geology*, **31**, 817–820.

XIAO, W. J., WINDLEY, B., HAO, J. & ZHAI, M. G. 2003. Accretion leading to collision and the Permian Solonker suture, Inner Mongolia, China: termination of the Central Asian Orogenic Belt. *Tectonics*, **22**(6), 1069, doi:10.1029/2002TC001484.

XU, J., MA, G., ZHU, G., TONG, W. X., GUI, K. R. & LIU, Q. 1987. Formation and evolution of the Tancheng–Lujiang wrench fault system: a major shear system to the northwest of the Pacific Ocean. *Tectonophysics*, **134**, 273–310.

XU, Y. G. 2001. Thermo-tectonic destruction of the Archaean lithospheric keel beneath the Sino-Korean Craton in China: evidence, timing and mechanism. *Physics and Chemistry of the Earth* (*A*), **26**, 747–758.

XU, Y. G., FAN, W. M. & LIN, G. 1995. Lithosphere–asthenosphere interaction: a comparative study on Cenozoic and Mesozoic basalts around Bohai Area. *Geotectonica et Metallogenica*, **19**, 1–13.

XU, Y. G., CHUNG, S. L., JAHN, B. M. & WU, G. Y. 2001. Petrologic and geochemical constraints on the petrogenesis of Permian–Triassic Emeishan flood basalts in southwestern China. *Lithos*, **58**, 145–168.

YANG, J. H., CHUNG, S. L., ZHAI, M. G. & ZHOU, X. H. 2004. Geochemical and Sr–Nd–Pb isotopic compositions of mafic dikes from the Jiaodong Peninsula, China: evidence for vein-plus-peridotite melting in the lithospheric mantle. *Lithos*, **73**, 145–160.

YIN, A. & NIE, S. 1993. An indentation model for the North and South China collision and the development of the Tan-Lu and Honam fault systems, eastern Asia. *Tectonics*, **12**, 801–813.

YING, J. F., ZHOU, X. H. & ZHANG, H. F. 2004. Geochemical and isotopic investigation of the Laiwu–Zibo carbonatites from western Shandong Province, China, and implications for their petrogenesis and enriched mantle source. *Lithos*, **75**, 413–426.

YOU, C.-F., CASTILLO, P. R., GIESKES, J. M., CHAN, L. H. & SPIVACK, A. J. 1996. Trace–element behavior in hydrothermal experiments: implications for fluid processes at shallow depths in subduction zones. *Earth and Planetary Science Letters*, **140**, 41–52.

ZHAI, M. G., BIAN, A. G. & ZHAO, T. P. 2000. The amalgamation of the supercontinent of North China Craton at the end of Neo-Archaean and its breakup during late Palaeoproterozoic and Mesoproterozoic. *Science in China* (*Series D*), **43**, 219–232.

ZHANG, G. H., ZHOU, X. H., SUN, M., CHEN, S. H. & FENG, J. L. 1998. Sr–Nd–Pb isotopic characteristics of granulite and pyroxenite xenoliths hosted in Cenozoic basalts from Hannuoba, Hebei Province and its geological significance. *Acta Petrologica Sinica*, **14**, 190–196 [in Chinese with English abstract].

ZHANG, H. F., SUN, M., ZHOU, X. H., FAN, W. M., ZHAI, M. G. & YING, J. F. 2002. Mesozoic lithosphere destruction beneath the North China Craton: evidence from major-, trace-element and Sr–Nd–Pb isotope

Downloaded from http://sp.lyellcollection.org/ at University of Sydney on May 1, 2015

studies of Fangcheng basalts. *Contributions to Mineralogy and Petrology*, **144**, 241–253.

ZHANG, H. F., SUN, M., ZHOU, X. H., ZHOU, M. F., FAN, W. M. & ZHENG, J. P. 2003. Secular evolution of the lithosphere beneath the eastern North China Craton: evidence from Mesozoic basalts and high-Mg andesites. *Geochimica et Cosmochimica Acta*, **67**, 4373–4387.

ZHANG, H. F., SUN, M., ZHOU, M. F., FAN, W. M., ZHOU, X. H. & ZHAI, M. G. 2004. Highly heterogeneous Late Mesozoic lithospheric mantle beneath the North China Craton: evidence from Sr–Nd–Pb isotopic systematics of mafic igneous rocks. *Geological Magazine*, **141**, 55–62.

ZHAO, G. C. 2001. Palaeoproterozoic assembly of the North China Craton. *Geological Magazine*, **138**, 87–91.

ZHAO, Y., YANG, Z. N. & MA, X. H. 1994. The important age of tectonic transformation from paleo-Asian to the Pacific tectonic domains in the East Asia. *Scientica Geologica Sinica*, **29**, 105–119 [in Chinese with English abstract].

ZHAO, Z. F., ZHENG, Y. F., WEI, C. S., WU, Y. B., CHEN, F. K. & JAHN, B. M. 2005. Zircon U–Pb age, element and C–O isotope geochemistry of post-collisional mafic–ultramafic rocks from the Dabie orogen in east–central China. *Lithos*, **83**, 1–28.

ZHENG, J. P., O'REILLY, S. Y., GRIFFIN, W. L., LU, F. X., ZHANG, M. & PEARSON, N. J. 2001. Relict refractory mantle beneath the eastern North China Block: significance for lithospheric evolution. *Lithos*, **57**, 43–66.

ZHENG, J. P., SUN, M., ZHOU, M. F. & ROBINSON, P. 2005. Trace elemental and PGE geochemical constraints of Mesozoic and Cenozoic peridotitic xenoliths on lithospheric evolution of the North China Craton. *Geochimica et Cosmochimica Acta*, **69**, 3401–3418.

ZHOU, X. H., ZHANG, G. H., YANG, J. H., CHEN, W. J. & SUN, M. 2001. Sr–Nd–Pb isotope mapping of late Mesozoic rocks across northern margin of North China Block and implications for geodynamic processes. *Geochimica*, **30**, 10–23 [in Chinese with English abstract].

ZHOU, X. H., SUN, M., ZHANG, G. H. & CHEN, S. H. 2002. Continental crust and lithospheric mantle interaction beneath North China: isotopic evidence from granulite xenoliths in Hannuoba, Sino-Korean craton. *Lithos*, **62**, 111–124.